

# Provably Consistent Partial-Label Learning

Lei Feng<sup>1\*</sup>, Jiaqi Lv<sup>2</sup>, Bo Han<sup>3,4</sup>, Miao Xu<sup>5,4</sup>,  
Gang Niu<sup>4</sup>, Xin Geng<sup>2</sup>, Bo An<sup>1</sup>, Masashi Sugiyama<sup>4,6</sup>

<sup>1</sup>Nanyang Technological University, Singapore

<sup>2</sup>Southeast University, China

<sup>3</sup>Hong Kong Baptist University, China

<sup>4</sup>RIKEN Center for Advanced Intelligence Project, Japan

<sup>5</sup>The University of Queensland, Australia

<sup>6</sup>The University of Tokyo, Japan

feng0093@e.ntu.edu.sg, boan@ntu.edu.sg

{lvjiaqi, xgeng}@seu.edu.cn

{bo.han, miao.xu, gang.niu}@riken.jp  
sugi@k.u-tokyo.ac.jp

## Abstract

*Partial-label learning* (PLL) is a multi-class classification problem, where each training example is associated with a *set of candidate labels*. Even though many practical PLL methods have been proposed in the last two decades, there lacks a theoretical understanding of the consistency of those methods—none of the PLL methods hitherto possesses a *generation process* of candidate label sets, and then it is still unclear why such a method works on a specific dataset and when it may fail given a different dataset. In this paper, we propose the first *generation model* of candidate label sets, and develop two novel PLL methods that are guaranteed to be provably consistent, i.e., one is *risk-consistent* and the other is *classifier-consistent*. Our methods are advantageous, since they are compatible with any deep network or stochastic optimizer. Furthermore, thanks to the generation model, we would be able to answer the two questions above by testing if the generation model matches given candidate label sets. Experiments on benchmark and real-world datasets validate the effectiveness of the proposed generation model and two PLL methods.

## 1 Introduction

Unlike supervised learning and unsupervised learning, weakly supervised learning [1] aims to learn with weak supervision. So far, various weakly supervised learning frameworks have been widely studied. Examples include *semi-supervised learning* [2, 3, 4], *multi-instance learning* [5, 6], *positive-unlabeled learning* [7, 8], *complementary-label learning* [9, 10], *noisy-label learning* [11, 12, 13], *positive-confidence learning* [14], *similar-unlabeled learning* [15], and *unlabeled-unlabeled learning* [16, 17].

In recent years, another weakly supervised learning framework called *partial-label learning* (PLL) [18, 19, 20, 21, 22, 23, 24] has gradually attracted attention from machine learning and data mining communities.

---

\*Preliminary work was done when Lei Feng was an intern at RIKEN AIP.

PLL aims to deal with the problem where each instance is provided with a set of candidate labels, only one of which is the correct label. In some studies, PLL is also termed as *ambiguous-label learning* [25, 26, 21, 27, 28] and *superset-label learning* [29, 20, 30]. Due to the difficulty in collecting accurately labeled data in many real-world scenarios, PLL has been successfully applied to a wide range of application domains, such as web mining [31], bird song classification [29], and automatic face naming [26].

A number of methods [18, 32, 22, 33, 23] have been proposed to improve the practical performance of PLL. On the theoretical side, some researchers have studied the statistical consistency [19] and learnability [20] of PLL. They made the same assumption on the *ambiguity degree*, which describes the maximum co-occurring probability of the correct label with another false positive label. Although they assumed that the data distribution for successful PLL should ensure a limited ambiguity degree, it is still unclear what the explicit formulation of the data distribution would be. Besides, the consistency of PLL methods would be hardly guaranteed without modeling the data distribution.

Motivated by the above observations, we for the first time present a novel statistical model to depict the generation process of partially labeled data. Having an explicit data distribution not only helps us to understand how partially labeled examples are generated, but also enables us to perform effective empirical risk minimization. Our proposed data generation model is instance-independent, which does not introduce any extra hidden variable. We verify that the proposed generation model satisfies the key assumption of PLL that the correct label is always included in the set of candidate labels.

Based on the data generation model, we further derive a novel *risk-consistent* method and a novel *classifier-consistent* method. Most of the existing PLL methods need to specially design complex optimization objectives, which make the optimization process inefficient. In contrast, our proposed PLL methods do not rely on specific classification models and can be easily trained with stochastic optimization, thus can be naturally applied to complex models such as deep neural networks with large-scale datasets. In addition, we theoretically derive an estimation error bound for each of the methods, which demonstrates that the obtained empirical risk minimizer would converge to the true risk minimizer as the number of training data tends to infinity. We show that the risk-consistent method holds a tighter estimation error bound than the classifier-consistent method and empirically validate that the risk-consistent method achieves better performance when deep neural networks are used. We also use *entropy* to measure how well the given candidate label sets match our generation model. We find that the candidate label sets with higher entropy better match our generation model, and on such datasets, our proposed PLL methods achieve better performance. Extensive experiments on benchmark as well as real-world partially labeled datasets clearly validate the effectiveness of our proposed methods.

## 2 Formulations

In this section, we introduce some notations and briefly review the formulations of learning with ordinary labels, learning with partial labels, and learning with complementary labels.

**Learning with Ordinary Labels.** For ordinary multi-class learning, let the feature space be  $\mathcal{X} \in \mathbb{R}^d$  and the label space be  $\mathcal{Y} = [k]$  (with  $k$  classes) where  $[k] := \{1, 2, \dots, k\}$ . Let us clearly define that  $\mathbf{x}$  denotes an instance and  $(\mathbf{x}, y)$  denotes an example including an instance  $\mathbf{x}$  and a label  $y$ . When ordinary labels are provided, we usually assume each example  $(\mathbf{x}, y) \in \mathcal{X} \times \mathcal{Y}$  is independently sampled from an unknown data distribution with probability density  $p(\mathbf{x}, y)$ . Then, the goal of multi-class learning is to obtain a multi-class classifier  $f : \mathcal{X} \rightarrow \mathbb{R}^k$  that minimizes the following classification risk:

$$R(f) = \mathbb{E}_{p(\mathbf{x}, y)}[\mathcal{L}(f(\mathbf{x}), y)], \quad (1)$$

where  $\mathbb{E}_{p(\mathbf{x},y)}[\cdot]$  denotes the expectation over the joint probability density  $p(\mathbf{x}, y)$  and  $\mathcal{L} : \mathbb{R}^k \times \mathcal{Y} \rightarrow \mathbb{R}_+$  is a multi-class loss function that measures how well a classifier estimates a given label. We say that a method is *classifier-consistent* if the learned classifier by the method is infinite-sample consistent to  $\arg \min_{f \in \mathcal{F}} R(f)$ , and a method is *risk-consistent* if the method possesses a classification risk estimator that is equivalent to  $R(f)$  given the same classifier  $f$ . It is worth noting that a risk-consistent method is also classifier-consistent [34]. However, a classifier-consistent method may not be risk-consistent.

**Learning with Partial Labels.** For learning with partial labels (i.e., PLL), each instance is provided with a set of candidate (partial) labels, only one of which is correct. Suppose the partially labeled dataset is denoted by  $\tilde{\mathcal{D}} = \{(\mathbf{x}_i, Y_i)\}_{i=1}^n$  where  $Y_i$  is the candidate label set of  $\mathbf{x}_i$ . Since each candidate label set should not be the empty set nor the whole label set, we have  $Y_i \in \mathcal{C}$  where  $\mathcal{C} = \{2^{\mathcal{Y}} \setminus \emptyset \setminus \mathcal{Y}\}$ ,  $2^{\mathcal{Y}}$  denotes the power set, and  $|\mathcal{C}| = 2^k - 2$ . The key assumption of PLL lies in that the correct label  $y_i$  of  $\mathbf{x}_i$  must be in the candidate label set, i.e.,

$$p(y_i \in Y_i \mid \mathbf{x}_i, Y_i) = 1, \quad \forall (\mathbf{x}_i, y_i) \in \mathcal{X} \times \mathcal{Y}, \quad \forall Y_i \in \mathcal{C}. \quad (2)$$

Given such data, the goal of PLL is to induce a multi-class classifier  $f : \mathcal{X} \rightarrow \mathbb{R}^k$  that can make correct predictions on test inputs. To this end, many methods [29, 22, 35, 30, 23, 24] have been proposed to improve the performance of PLL. However, to the best of our knowledge, there is only one method [19] that possesses statistical consistency by providing a classifier-consistent risk estimator. However, it not only requires the assumption that the data distribution should ensure a limited ambiguity degree, but also relies on some strict conditions (e.g., convexity of loss function and dominance relation [19]). It is still unclear what the explicit formulation of the data distribution for successful PLL would be. Besides, it is also unknown whether there exists a risk-consistent method that possesses a statistical unbiased estimator of the classification risk  $R(f)$ .

**Learning with Complementary Labels.** There is a special case of partial labels, called complementary labels [9, 36, 10]. Each complementary label specifies one of the classes that the example does *not* belong to. Hence a complementary label  $\bar{y}$  can be considered as an extreme case where all  $k - 1$  classes other than the class  $\bar{y}$  are taken as candidate (partial) labels. Existing studies on learning with complementary labels make the assumption on the data generation process. The pioneering study [9] assumed that each complementarily labeled example  $(\mathbf{x}, \bar{y})$  is independently drawn from the probability distribution with density  $\bar{p}(\mathbf{x}, y)$ , where  $\bar{p}(\mathbf{x}, y)$  is defined as  $\bar{p}(\mathbf{x}, \bar{y}) = \sum_{y \neq \bar{y}} p(\mathbf{x}, y)$ . Based on this data distribution, several risk-consistent methods [9, 10] have been proposed for learning with complementary labels. However, in many real-world scenarios, multiple complementary labels would be more widespread than a single complementary label. Hence a recent study [37] focused on learning with multiple complementary labels. Suppose each training example is represented by  $(\mathbf{x}, \bar{Y})$  where  $\bar{Y}$  denotes a set of multiple complementary labels, and  $(\mathbf{x}, \bar{Y})$  is assumed to be independently sampled from the probability distribution with density  $\bar{p}(\mathbf{x}, \bar{Y})$ , which is defined as

$$\bar{p}(\mathbf{x}, \bar{Y}) = \sum_{j=1}^{k-1} p(s = j) \bar{p}(\mathbf{x}, \bar{Y} \mid s = j), \quad (3)$$

where

$$\bar{p}(\mathbf{x}, \bar{Y} \mid s = j) := \begin{cases} \frac{1}{\binom{k-1}{j}} \sum_{y \notin \bar{Y}} p(\mathbf{x}, y) & \text{if } |\bar{Y}| = j, \\ 0 & \text{otherwise.} \end{cases} \quad (4)$$

Here, the variable  $s$  denotes the size of the complementary label set. Supplied with this data distribution, a risk-consistent method [37] was proposed. It is worth noting that following the distribution of complementarily labeled data, although we can obtain partial labels by regarding all the complementary labels as non-candidate

labels, the resulting distribution of partially labeled data is not explicitly formulated. It would be natural to ask whether there also exists an explicit formulation of the partially labeled data distribution that enables us to derive a novel classifier-consistent method or a novel risk-consistent method that possesses statistical consistency. In this paper, we will give an affirmative answer to this question. Specifically, we will show that based on our proposed data generation model, a novel risk-consistent method (the first one for PLL) and a novel classifier-consistent method can be derived accordingly.

### 3 Data Generation Model

In this section, we present an explicit formulation of the generation process of partially labeled data, and show that it satisfies the key assumption (i.e., Eq. (2)) of PLL.

#### 3.1 Partially Labeled Data Distribution

We assume each partially labeled example  $(\mathbf{x}, Y)$  is independently drawn from a probability distribution with the following density:

$$\tilde{p}(\mathbf{x}, Y) = \sum_{i=1}^k p(Y | y = i)p(\mathbf{x}, y = i), \text{ where } p(Y | y = i) = \begin{cases} \frac{1}{2^{k-1}-1} & \text{if } i \in Y, \\ 0 & \text{if } i \notin Y. \end{cases} \quad (5)$$

In Eq. (5), we assume  $p(Y | \mathbf{x}, y) = p(Y | y)$ , which means, given the correct label  $y$ , the candidate label set  $Y$  is independent of the instance  $\mathbf{x}$ . This assumption is similar to the conventional modeling of label noise [38] where the observed noisy label is independent of the instance, given the correct label. In addition, there are in total  $2^{k-1} - 1$  possible candidate label sets that contain a specific label  $y$ . Hence, Eq. (5) describes the probability of each candidate label set being uniformly sampled, given a specific label. Here, we show that our assumed data distribution is a valid probability distribution by the following theorem.

**Theorem 1.** *The equality  $\int_{\mathcal{C}} \int_{\mathcal{X}} \tilde{p}(\mathbf{x}, Y) d\mathbf{x} dY = 1$  holds.*

The proof is provided in Appendix A.1. Given the assumed data distribution in Eq. (5), it would be natural to ask whether our assumed data distribution meets the key assumption of PLL described in Eq. (2), i.e., whether the correct label  $y$  is always in the candidate label set  $Y$  for every partially labeled example  $(\mathbf{x}, Y)$  sampled from  $\tilde{p}(\mathbf{x}, Y)$ . The following theorem provides an affirmative answer to this question.

**Theorem 2.** *For any partially labeled example  $(\mathbf{x}, Y)$  independently sampled from the assumed data distribution in Eq. (5), the correct label  $y$  is always in the candidate label set  $Y$ , i.e.,  $p(y \in Y | \mathbf{x}, Y) = 1, \forall (\mathbf{x}, Y) \sim \tilde{p}(\mathbf{x}, Y)$ .*

The proof is provided in Appendix A.2. Theorem 2 clearly demonstrates that our assumed data distribution in Eq. (5) satisfies the key assumption of PLL.

#### 3.2 Motivation

Here, we provide a motivation why we derived the above data generation model.

Generally, a large number of high-quality samples are notably helpful to machine learning or data mining. However, it is usually difficult for our labelers to directly identify the correct label for each instance [1]. Nonetheless, it would be easier to collect a set of candidate labels that contains the correct label. Suppose there is a labeling system that can uniformly sample a label set  $Y$  from  $\mathcal{C}$ . For each instance  $\mathbf{x}$ , the labeling system uniformly samples a label set  $Y$  and asks a labeler whether the correct label  $y$  is in the sampled label set  $Y$ . In this case, the collected examples whose correct label  $y$  is included in the proposed label set  $Y$  follow the same distribution as Eq. (5). In order to justify that, we first introduce the following lemma.

**Lemma 1.** *Given any instance  $\mathbf{x}$  with its correct label  $y$ , for any unknown label set  $Y$  that is uniformly sampled from  $\mathcal{C}$ , the equality  $p(y \in Y \mid \mathbf{x}) = 1/2$  holds.*

It is quite intuitive to verify that Lemma 1 indeed holds. Specifically, if we do not have any information of  $Y$ , we may randomly guess with even probabilities whether the correct  $y$  is included in an unknown label set  $Y$  or not. A rigorous mathematical proof is provided in Appendix A.3. Based on Lemma 1, we have the following theorem.

**Theorem 3.** *In the above setting, the distribution of the collected data whose correct label  $y \in \mathcal{Y}$  is included in the label set  $Y \in \mathcal{C}$  is the same as Eq. (5), i.e.,  $p(\mathbf{x}, Y \mid y \in Y) = \tilde{p}(\mathbf{x}, Y)$  where  $\tilde{p}(\mathbf{x}, Y)$  is defined in Eq. (5).*

The proof is provided in Appendix A.4.

## 4 Consistent Methods

In this section, based on our assumed partially labeled data distribution in Eq. (5), we present a novel risk-consistent method and a novel classifier-consistent method, and theoretically derive an estimator error bound for each of them. Both of the consistent methods are agnostic in specific classification models and can be easily trained with stochastic optimization, which ensures their scalability to large-scale datasets.

### 4.1 Risk-Consistent Method

For the risk-consistent method, we employ the *importance reweighting* strategy [39] to rewrite the classification risk  $R(f)$  as

$$\begin{aligned}
R(f) &= \mathbb{E}_{p(\mathbf{x}, y)}[\mathcal{L}(f(\mathbf{x}), y)] = \int_{\mathbf{x}} \sum_{i=1}^k p(y = i \mid \mathbf{x}) \mathcal{L}(f(\mathbf{x}), i) p(\mathbf{x}) d\mathbf{x} \\
&= \int_{\mathbf{x}} \sum_{i=1}^k \frac{1}{|\mathcal{C}|} \sum_{Y \in \mathcal{C}} p(Y \mid \mathbf{x}) \frac{p(y=i|\mathbf{x})}{p(Y|\mathbf{x})} \mathcal{L}(f(\mathbf{x}), i) p(\mathbf{x}) d\mathbf{x} \\
&= \frac{1}{|\mathcal{C}|} \int_{\mathbf{x}} \sum_{Y \in \mathcal{C}} p(Y \mid \mathbf{x}) \left[ \sum_{i=1}^k \frac{p(y=i|\mathbf{x})}{p(Y|\mathbf{x})} \mathcal{L}(f(\mathbf{x}), i) \right] p(\mathbf{x}) d\mathbf{x} \\
&= \frac{1}{2^k - 2} \mathbb{E}_{\tilde{p}(\mathbf{x}, Y)} \left[ \sum_{i=1}^k \frac{p(y=i|\mathbf{x})}{p(Y|\mathbf{x})} \mathcal{L}(f(\mathbf{x}), i) \right] = R_{\text{rc}}(f).
\end{aligned} \tag{6}$$

Here,  $p(Y \mid \mathbf{x})$  can be calculated by

$$p(Y \mid \mathbf{x}) = \sum_{j=1}^k p(Y \mid y = j) p(y = j \mid \mathbf{x}) = \frac{1}{2^{k-1} - 1} \sum_{j \in Y} p(y = j \mid \mathbf{x}), \tag{7}$$

where the last equality holds due to Eq. (5). By substituting Eq. (7) into Eq. (6), we obtain

$$R_{\text{rc}}(f) = \frac{1}{2} \mathbb{E}_{\tilde{p}(\mathbf{x}, Y)} \left[ \sum_{i=1}^k \frac{p(y=i|\mathbf{x})}{\sum_{j \in Y} p(y=j|\mathbf{x})} \mathcal{L}(f(\mathbf{x}), i) \right]. \tag{8}$$

In this way, its empirical risk estimator can be expressed as

$$\widehat{R}_{\text{rc}}(f) = \frac{1}{2n} \sum_{o=1}^n \left( \sum_{i=1}^k \frac{p(y_o=i|\mathbf{x}_o)}{\sum_{j \in Y_o} p(y_o=j|\mathbf{x}_o)} \mathcal{L}(f(\mathbf{x}_o), i) \right), \tag{9}$$

where  $\{\mathbf{x}_o, Y_o\}_{o=1}^n$  are partially labeled examples drawn from  $\tilde{p}(\mathbf{x}, Y)$ . Note that  $p(y = i \mid \mathbf{x})$  is not accessible from the given data. Therefore, we apply the softmax function on the model output  $f(\mathbf{x})$  to approximate  $p(y = i \mid \mathbf{x})$ , i.e.,  $p(y = i \mid \mathbf{x}) = g_i(\mathbf{x})$  where  $g_i(\mathbf{x})$  is the probability of label  $i$  being the true label of  $\mathbf{x}$ , which is calculated by  $g_i(\mathbf{x}) = \exp(f_i(\mathbf{x})) / \sum_{j=1}^k \exp(f_j(\mathbf{x}))$ , and  $f_i(\mathbf{x})$  is the  $i$ -th coordinate of  $f(\mathbf{x})$ . It is worth

noting that the non-candidate labels can never be the correct label. Therefore, we further correct  $p(y = i | \mathbf{x})$  by setting the confidence of each non-candidate label to 0, i.e.,

$$p(y = i | \mathbf{x}) = g_i(\mathbf{x}) \text{ if } i \in Y, \text{ otherwise } p(y = i | \mathbf{x}) = 0, \forall (\mathbf{x}, Y) \sim \tilde{p}(\mathbf{x}, Y). \quad (10)$$

As shown in Eq. (9), our risk-consistent method does not rely on specific loss functions, hence we simply adopt the widely-used categorical cross entropy loss for practical implementation. The pseudo-code of the Risk-Consistent (RC) method is presented in Algorithm 1.

Here, we establish an estimation error bound for the risk-consistent method. Specifically, let  $\hat{f}_{\text{rc}} = \min_{f \in \mathcal{F}} \hat{R}_{\text{rc}}(f)$  be the empirical risk minimizer and  $f^* = \min_{f \in \mathcal{F}} R(f)$  be the true risk minimizer. Besides, we define the function space  $\mathcal{H}_y$  for the label  $y \in \mathcal{Y}$  as  $\{h : \mathbf{x} \mapsto f_y(\mathbf{x}) \mid f \in \mathcal{F}\}$ . Let  $\mathfrak{R}_n(\mathcal{H}_y)$  be the expected Rademacher complexity [40] of  $\mathcal{H}_y$  with sample size  $n$ , then we have the following theorem.

**Theorem 4.** *Assume the loss function  $\mathcal{L}(f(\mathbf{x}), y)$  is  $\rho$ -Lipschitz with respect to  $f_y(\mathbf{x})$  ( $0 < \rho < \infty$ ) for all  $y \in \mathcal{Y}$  and upper-bounded by  $M$ , i.e.,  $M = \sup_{\mathbf{x} \in \mathcal{X}, f \in \mathcal{F}, y \in \mathcal{Y}} \mathcal{L}(f(\mathbf{x}), y)$ . Then, for any  $\delta > 0$ , with probability at least  $1 - \delta$ ,*

$$R(\hat{f}_{\text{rc}}) - R(f^*) \leq 4\rho \sum_{y=1}^k \mathfrak{R}_n(\mathcal{H}_y) + M \sqrt{\frac{\log \frac{2}{\delta}}{2n}},$$

The proof of Theorem 4 is provided in Appendix B. Generally,  $\mathfrak{R}_n(\mathcal{H}_y)$  can be bounded by  $C_{\mathcal{H}}/\sqrt{n}$  for a positive constant  $C_{\mathcal{H}}$  [17, 34, 41]. Hence Theorem 4 shows that the empirical risk minimizer  $\hat{f}_{\text{rc}}$  converges to the true risk minimizer  $f^*$  as  $n \rightarrow \infty$ .

## 4.2 Classifier-Consistent Method

For the classifier-consistent method, we start by introducing a transition matrix  $\mathbf{Q}$  that describes the probability of the candidate label set given an ordinary label. Specifically, the transition matrix  $\mathbf{Q}$  is defined as  $Q_{ij} = p(C_j | y = i)$  where  $C_j \in \mathcal{C}$  ( $j \in [2^k - 2]$ ) is a specific label set. By further taking into account the assumed data distribution in Eq. (5), we can instantiate the transition matrix  $\mathbf{Q}$  as  $Q_{ij} = \frac{1}{2^{k-1}-1}$  if  $i \in C_j$ , otherwise  $Q_{ij} = 0$ . Let us introduce  $q_j(\mathbf{x}) = p(Y = C_j | \mathbf{x})$  and  $g_i(\mathbf{x}) = p(y = i | \mathbf{x})$ , then we can obtain  $q(\mathbf{x}) = \mathbf{Q}^\top g(\mathbf{x})$ .

Given each partially labeled example  $(\mathbf{x}, Y)$  sampled from  $\tilde{p}(\mathbf{x}, Y)$ , the proposed classifier-consistent risk estimator is presented as

$$R_{\text{cc}}(f) = \mathbb{E}_{\tilde{p}(\mathbf{x}, Y)}[\mathcal{L}(q(\mathbf{x}), \tilde{y})], \text{ where } C_{\tilde{y}} = Y. \quad (11)$$

In this formulation, we regard the candidate label set  $Y$  as a virtual label  $\tilde{y}$  if  $Y$  is a specific label set  $C_{\tilde{y}}$ . Since there are  $2^k - 2$  possible label sets, we denote by  $\tilde{\mathcal{Y}}$  the virtual label space where  $\tilde{\mathcal{Y}} = [2^k - 2]$  and  $\tilde{y} \in \tilde{\mathcal{Y}}$ . In order to prove that this method is classifier-consistent, we introduce the following two lemmas.

**Lemma 2.** *The transition matrix  $\mathbf{Q}$  is invertible.*

The proof is provided in Appendix C.1.

**Lemma 3.** *If certain loss functions are used (e.g., the softmax cross entropy loss or mean squared error), the optimal mapping  $g^*$  satisfies  $g_i^*(\mathbf{x}) = p(y = i | \mathbf{x})$ .*

The proof is provided in Appendix C.2. The same proof can be found in [36, 42].

**Theorem 5.** *With the conditions in Lemma 2 and Lemma 3 satisfied, the minimizer  $f_{\text{cc}} = \arg \min_{f \in \mathcal{F}} R_{\text{cc}}(f)$  is also the true minimizer  $f^* = \arg \min_{f \in \mathcal{F}} R(f)$ , i.e.,  $f_{\text{cc}} = f^*$  (classifier-consistency).*

---

**Algorithm 1** RC Algorithm

---

**Input:** Model  $f$ , epoch  $T_{\max}$ , iteration  $I_{\max}$ , partially labeled training set  $\tilde{\mathcal{D}} = \{(\mathbf{x}_i, Y_i)\}_{i=1}^n$ .

- 1: **Initialize**  $p(y_i = j | \mathbf{x}_i) = 1, \forall j \in Y_i$ , otherwise  $p(y_i = j | \mathbf{x}_i) = 0$ ;
- 2: **for**  $t = 1, 2, \dots, T_{\max}$  **do**
- 3:     **Shuffle**  $\tilde{\mathcal{D}} = \{(\mathbf{x}_i, Y_i)\}_{i=1}^n$ ;
- 4:     **for**  $j = 1, \dots, I_{\max}$  **do**
- 5:         **Fetch** mini-batch  $\tilde{\mathcal{D}}_j$  from  $\tilde{\mathcal{D}}$ ;
- 6:         **Update** model  $f$  by  $\hat{R}_{\text{rc}}$  in Eq. (9);
- 7:         **Update**  $p(y_i | \mathbf{x}_i)$  by Eq. (10);
- 8:     **end for**
- 9: **end for**

**Output:**  $f$ .

---

---

**Algorithm 2** CC Algorithm

---

**Input:** Model  $f$ , epoch  $T_{\max}$ , iteration  $I_{\max}$ , partially labeled training set  $\tilde{\mathcal{D}} = \{(\mathbf{x}_i, Y_i)\}_{i=1}^n$ ;

- 1: **for**  $t = 1, 2, \dots, T_{\max}$  **do**
- 2:     **Shuffle** the partially labeled training set  $\tilde{\mathcal{D}} = \{(\mathbf{x}_i, Y_i)\}_{i=1}^n$ ;
- 3:     **for**  $j = 1, \dots, I_{\max}$  **do**
- 4:         **Fetch** mini-batch  $\tilde{\mathcal{D}}_j$  from  $\tilde{\mathcal{D}}$ ;
- 5:         **Update** model  $f$  by minimizing the empirical risk estimator  $\hat{R}_{\text{cc}}$  in Eq. (12);
- 6:     **end for**
- 7: **end for**

**Output:**  $f$ .

---

The proof is provided in Appendix C.3.

As suggested by Lemma 3, we adopt the softmax cross entropy loss in our classifier-consistent risk estimator (i.e., Eq. (11)) for practical implementation. In this way, we have the following empirical risk estimator:

$$\begin{aligned} \hat{R}_{\text{cc}}(f) &= -\frac{1}{n} \sum_{i=1}^n \left( \sum_{j=1}^{2^k-2} \mathbb{I}(Y_i = C_j) \log(q_j(\mathbf{x}_i)) \right) = -\frac{1}{n} \sum_{i=1}^n \sum_{j=1}^{2^k-2} \mathbb{I}(Y_i = C_j) \log(\mathbf{Q}[:, j]^\top g(\mathbf{x})) \\ &= -\frac{1}{n} \sum_{i=1}^n \log \left( \frac{1}{2^{k-1}-1} \sum_{y \in Y_i} g_y(\mathbf{x}) \right) = -\frac{1}{n} \sum_{i=1}^n \log \left( \frac{1}{2^{k-1}-1} \sum_{y \in Y_i} \frac{\exp(f_y(\mathbf{x}))}{\sum_j \exp(f_j(\mathbf{x}))} \right), \end{aligned} \quad (12)$$

where  $\mathbb{I}[\cdot]$  is the indicator function. For the expected risk estimator  $R_{\text{cc}}(f)$ , it seems that the transition matrix  $\mathbf{Q} \in \mathbb{R}^{k \times (2^k-2)}$  is indispensable. Unfortunately, it would be computationally prohibitive, since  $2^k - 2$  is an extremely large number if the number of classes  $k$  is large. However, for practical implementation, Eq. (12) shows that we do not need to explicitly calculate and store the transition matrix  $\mathbf{Q}$ , which brings no pain to optimization. The pseudo-code of the Classifier-Consistent (CC) method is presented in Algorithm 2.

Here, we also establish an estimation error bound for the classifier-consistent method. Let  $\hat{f}_{\text{cc}} = \arg \min_{f \in \mathcal{F}} \hat{R}_{\text{cc}}(f)$  be the empirical minimizer and  $f^* = \arg \min_{f \in \mathcal{F}} R(f)$  be the true minimizer. Besides, we define the function space  $\mathcal{H}_y$  for the label  $y \in \mathcal{Y}$  as  $\{h : \mathbf{x} \mapsto f_y(\mathbf{x}) \mid f \in \mathcal{F}\}$ . Then, we have the following theorem.

**Theorem 6.** *Assume the loss function  $\mathcal{L}(q(\mathbf{x}), \tilde{y})$  is  $\rho'$ -Lipschitz with respect to  $f_y(\mathbf{x})$  ( $0 < \rho < \infty$ ) for all  $y \in \mathcal{Y}$  and upper-bounded by  $M$ , i.e.,  $M = \sup_{\mathbf{x} \in \mathcal{X}, f \in \mathcal{F}, \tilde{y} \in \tilde{\mathcal{Y}}} \mathcal{L}(q(\mathbf{x}), \tilde{y})$ . Then, for any  $\delta > 0$ , with probability*

at least  $1 - \delta$ ,

$$R_{\text{cc}}(\hat{f}_{\text{cc}}) - R_{\text{cc}}(f^*) \leq 8\rho' \sum_{y=1}^k \mathfrak{R}_n(\mathcal{H}_y) + 2M \sqrt{\frac{\log \frac{2}{\delta}}{2n}}.$$

The proof is provided in Appendix D. Generally,  $\mathfrak{R}_n(\mathcal{H}_y)$  can be bounded by  $C_{\mathcal{H}}/\sqrt{n}$  for a positive constant  $C_{\mathcal{H}}$  [17, 34, 41]. Hence Theorem 6 demonstrates that the empirical risk minimizer  $\hat{f}_{\text{cc}}$  converges to the true risk minimizer  $f^*$  as  $n \rightarrow \infty$ .

**Theoretical Comparison Between RC and CC.** It is worth noting that the difference of the estimation error bounds in Theorem 4 and Theorem 6 mainly comes from the first term, since there only exists a constant difference in the second term even though various models are used. If we assume that  $\rho$  for RC and  $\rho'$  for CC hold the same value, we can find that the estimation error bound in Theorem 6 could be notably looser than that in Theorem 4 when the Rademacher complexity of the model class is large. This observation suggests that RC probably achieves smaller estimation error than CC when complex models are used. We will demonstrate via experiments that RC generally outperforms CC when deep neural networks are used.

## 5 Experiments

In this section, we conduct extensive experiments on various datasets to validate the effectiveness of our proposed methods.

**Datasets.** We collect four widely used benchmark datasets including MNIST [43], Kuzushiji-MNIST [44], Fashion-MNIST [45], and CIFAR-10 [46], and five datasets from the UCI Machine Learning Repository [46]. In order to generate candidate label sets on these datasets, following the motivation in Section 3.2, we uniformly sample the candidate label set that includes the correct label from  $\mathcal{C}$  for each instance. In addition, we also use five widely used real-world partially labeled datasets, including Lost [19], BirdSong [47], MSRCv2 [29], Soccer Player [26], Yahoo! News [48]. Since our proposed methods do not rely on specific classification models, we use various base models to validate the effectiveness of our methods, including linear model, three-layer ( $d$ -500- $k$ ) MLP, 5-layer LeNet, 34-layer ResNet [49], and 22-layer DenseNet [50]. The detailed descriptions of these datasets with the corresponding base models are provided in Appendix E.1.

**Compared Methods.** We compare with six state-of-the-art PLL methods including SURE [23], CLPL [19], IPAL [22], PLSVM [51], PLECO [35], PLkNN [25]. Besides, we also compare with various *complementary-label learning* (CLL) methods for two reasons: 1) We can directly use CLL methods on partially labeled datasets by regarding non-candidate labels as complementary labels. 2) Existing CLL methods can be applied to large-scale datasets. The compared CLL methods include GA, NN, and Free [10], PC [9], Forward [36], the unbiased risk estimator [37] with bounded losses MAE, MSE, GCE, Phuber-CE, and the surrogate losses EXP and LOG. For all the above methods, their hyper-parameters are specified or searched according to the suggested parameter settings by respective papers. The detailed information of these compared methods is provided in Appendix E.2. For our proposed methods RC (Algorithm 1) and CC (Algorithm 2), we only need to search learning rate and weight decay from  $\{10^{-6}, \dots, 10^{-1}\}$ , since there are no other hyper-parameters in our methods. Hyper-parameters are selected so as to maximize the accuracy on a validation set (10% of the training set) of partially labeled data. We implement them using PyTorch [52] and use the Adam [53] optimizer with the mini-batch size set to 256 and the number of epochs set to 250.

**Experimental Results.** We run 5 trials on the four benchmark datasets and run 10 trials (with 90%/10% train/test split) on UCI datasets and real-world partially labeled datasets, and record the mean accuracy with standard deviation (mean $\pm$ std). We also use paired  $t$ -test at 5% significance level, and  $\bullet/\circ$  represents whether the *best* of RC and CC is significantly better/worse than other compared methods. Besides, the best results are highlighted in bold. Tabel 1 and Table 2 report the test performance of each method using

Table 1: Test performance (mean $\pm$ std) of each method using neural networks on benchmark datasets. ResNet is trained on CIFAR-10, and MLP is trained on the other three datasets.

	MNIST	Kuzushiji-MNIST	Fashion-MNIST	CIFAR-10
RC	<b>98.00<math>\pm</math>0.11%</b>	<b>89.38<math>\pm</math>0.28%</b>	<b>88.38<math>\pm</math>0.16%</b>	<b>77.93<math>\pm</math>0.59%</b>
CC	97.87 $\pm$ 0.10%●	88.83 $\pm$ 0.40%●	87.88 $\pm$ 0.25%●	75.78 $\pm$ 0.27%●
GA	96.37 $\pm$ 0.13%●	84.23 $\pm$ 0.19%●	85.57 $\pm$ 0.16%●	72.22 $\pm$ 0.19%●
NN	96.75 $\pm$ 0.08%●	82.36 $\pm$ 0.41%●	86.25 $\pm$ 0.14%●	68.09 $\pm$ 0.31%●
Free	88.48 $\pm$ 0.37%●	70.31 $\pm$ 0.68%●	81.34 $\pm$ 0.47%●	17.74 $\pm$ 1.20%●
PC	92.47 $\pm$ 0.13%●	73.45 $\pm$ 0.20%●	83.37 $\pm$ 0.31%●	46.53 $\pm$ 2.01%●
Forward	97.64 $\pm$ 0.11%●	87.64 $\pm$ 0.13%●	86.73 $\pm$ 0.15%●	71.18 $\pm$ 0.92%●
EXP	97.81 $\pm$ 0.04%●	88.48 $\pm$ 0.29%●	87.96 $\pm$ 0.06%●	73.22 $\pm$ 0.66%●
LOG	97.86 $\pm$ 0.11%●	88.24 $\pm$ 0.08%●	88.31 $\pm$ 0.26%	75.38 $\pm$ 0.34%●
MAE	97.82 $\pm$ 0.11%●	88.43 $\pm$ 0.32%●	87.83 $\pm$ 0.22%●	66.91 $\pm$ 3.08%●
MSE	96.95 $\pm$ 0.14%●	85.16 $\pm$ 0.44%●	85.72 $\pm$ 0.26%●	66.15 $\pm$ 2.13%●
GCE	96.71 $\pm$ 0.08%●	85.19 $\pm$ 0.39%●	86.88 $\pm$ 0.16%●	68.39 $\pm$ 0.71%●
Phuber-CE	95.10 $\pm$ 0.34%●	80.66 $\pm$ 0.41%●	85.33 $\pm$ 0.23%●	58.60 $\pm$ 0.95%●

Table 2: Test performance (mean $\pm$ std) of each method using neural networks on benchmark datasets. DenseNet is trained on CIFAR-10, and LeNet is trained on the other three datasets.

	MNIST	Kuzushiji-MNIST	Fashion-MNIST	CIFAR-10
RC	<b>99.04<math>\pm</math>0.03%</b>	<b>94.00<math>\pm</math>0.30%</b>	<b>89.48<math>\pm</math>0.15%</b>	<b>78.53<math>\pm</math>0.46%</b>
CC	98.99 $\pm$ 0.08%	93.86 $\pm$ 0.18%	88.98 $\pm$ 0.20%●	75.71 $\pm$ 0.18%●
GA	98.68 $\pm$ 0.05%●	90.39 $\pm$ 0.26%●	87.95 $\pm$ 0.12%●	71.85 $\pm$ 0.19%●
NN	98.51 $\pm$ 0.08%●	89.60 $\pm$ 0.34%●	88.47 $\pm$ 0.15%●	71.98 $\pm$ 0.35%●
Free	80.48 $\pm$ 2.06%●	71.18 $\pm$ 1.38%●	74.02 $\pm$ 3.88%●	45.94 $\pm$ 0.83%●
PC	95.03 $\pm$ 0.16%●	79.62 $\pm$ 0.11%●	83.98 $\pm$ 0.20%●	54.18 $\pm$ 2.10%●
Forward	98.80 $\pm$ 0.04%●	93.87 $\pm$ 0.14%	88.72 $\pm$ 0.17%●	73.56 $\pm$ 1.47%●
EXP	98.82 $\pm$ 0.03%●	92.69 $\pm$ 0.31%●	88.99 $\pm$ 0.25%●	75.02 $\pm$ 1.02%●
LOG	98.88 $\pm$ 0.08%●	93.97 $\pm$ 0.25%	88.75 $\pm$ 0.28%●	75.54 $\pm$ 0.59%●
MAE	98.88 $\pm$ 0.05%●	93.04 $\pm$ 0.52%●	87.30 $\pm$ 3.16%●	67.74 $\pm$ 0.89%●
MSE	98.38 $\pm$ 0.05%●	88.37 $\pm$ 0.55%●	88.18 $\pm$ 0.08%●	70.66 $\pm$ 0.59%●
GCE	98.63 $\pm$ 0.06%●	91.27 $\pm$ 0.30%●	88.66 $\pm$ 0.16%●	72.09 $\pm$ 0.51%●
Phuber-CE	96.92 $\pm$ 0.18%●	82.24 $\pm$ 2.45%●	87.02 $\pm$ 0.09%●	66.47 $\pm$ 0.35%●

Table 3: Test performance (mean $\pm$ std) of each method using linear model on UCI datasets.

	Texture	Yeast	Dermatology	Har	20Newsgroups
RC	99.24 $\pm$ 0.14%	59.89 $\pm$ 1.27%	99.41 $\pm$ 1.00%	98.03 $\pm$ 0.09%	<b>75.99<math>\pm</math>0.53%</b>
CC	98.02 $\pm$ 2.91%●	<b>59.97<math>\pm</math>1.57%</b>	<b>99.73<math>\pm</math>0.85%</b>	<b>98.10<math>\pm</math>0.18%</b>	75.97 $\pm$ 0.54%
SURE	95.38 $\pm$ 0.28%●	54.39 $\pm$ 1.32%●	97.48 $\pm$ 0.32%●	97.43 $\pm$ 0.24%●	69.82 $\pm$ 0.26%●
CLPL	91.93 $\pm$ 0.97%●	54.58 $\pm$ 2.11%●	99.62 $\pm$ 0.85%	97.48 $\pm$ 0.18%●	71.44 $\pm$ 0.55%●
PLECOC	69.69 $\pm$ 4.82%●	37.37 $\pm$ 9.73%●	87.84 $\pm$ 5.30%●	96.97 $\pm$ 0.29%●	15.32 $\pm$ 7.86%●
PLSVM	49.38 $\pm$ 9.99%●	45.70 $\pm$ 8.01%●	80.00 $\pm$ 7.53%●	91.64 $\pm$ 1.43%●	32.59 $\pm$ 8.91%●
PL $k$ NN	96.78 $\pm$ 0.31%●	47.79 $\pm$ 2.41%●	80.54 $\pm$ 5.06%●	94.17 $\pm$ 0.59%●	27.18 $\pm$ 0.65%●
IPAL	<b>99.45<math>\pm</math>0.23%</b>	48.99 $\pm$ 3.84%●	98.65 $\pm$ 2.27%●	96.55 $\pm$ 0.40%●	48.36 $\pm$ 0.85%●

neural networks on benchmark datasets. We also provide the transductive performance of each method in Appendix E.3. From the two tables, we can observe that RC always achieves the best performance and

Table 4: Test performance (mean $\pm$ std) of each method using linear model on real-world datasets.

	Lost	MSRCv2	BirdSong	Soccer Player	Yahoo! News
RC	<b>79.43<math>\pm</math>3.26%</b>	46.56 $\pm$ 2.71%	71.94 $\pm$ 1.72%	<b>57.00<math>\pm</math>0.97%</b>	<b>68.23<math>\pm</math>0.83%</b>
CC	79.29 $\pm$ 3.19%	47.22 $\pm$ 3.02%	<b>72.22<math>\pm</math>1.71%</b>	56.32 $\pm$ 0.64%	68.14 $\pm$ 0.81%
SURE	71.33 $\pm$ 3.57% $\bullet$	46.88 $\pm$ 4.67%	58.92 $\pm$ 1.28% $\bullet$	49.41 $\pm$ 0.86% $\bullet$	45.49 $\pm$ 1.15% $\bullet$
CLPL	74.87 $\pm$ 4.30% $\bullet$	36.53 $\pm$ 4.59% $\bullet$	63.56 $\pm$ 1.40% $\bullet$	36.82 $\pm$ 1.04% $\bullet$	46.21 $\pm$ 0.90% $\bullet$
PLECOC	49.03 $\pm$ 8.36% $\bullet$	41.53 $\pm$ 3.25% $\bullet$	71.58 $\pm$ 1.81%	53.70 $\pm$ 2.02% $\bullet$	66.22 $\pm$ 1.01% $\bullet$
PLSVM	75.31 $\pm$ 3.81% $\bullet$	35.85 $\pm$ 4.41% $\bullet$	49.90 $\pm$ 2.07% $\bullet$	46.29 $\pm$ 0.96% $\bullet$	56.85 $\pm$ 0.91% $\bullet$
PL $k$ NN	36.73 $\pm$ 2.99% $\bullet$	41.36 $\pm$ 2.89% $\bullet$	64.94 $\pm$ 1.42% $\bullet$	49.62 $\pm$ 0.67% $\bullet$	41.07 $\pm$ 1.02% $\bullet$
IPAL	72.12 $\pm$ 4.48% $\bullet$	<b>50.80<math>\pm</math>4.46%</b> $\circ$	72.06 $\pm$ 1.55%	55.03 $\pm$ 0.77% $\bullet$	66.79 $\pm$ 1.22% $\bullet$

significantly outperforms other compared methods in most cases. In addition, we record the test accuracy at each training epoch to provide more detailed visualized results in Appendix E.4. Table 3 and Table 4 report the test performance of each method using linear model on UCI datasets and real-world partially labeled datasets, respectively. We can find that RC and CC generally achieve superior performance against other compared methods on both UCI datasets and real-world partially labeled datasets.

**Performance Comparison Between RC and CC.** It can be seen that when linear model is used, RC and CC achieve similar performance. However, RC significantly outperforms CC when deep neural networks are used. These observations accord with our derived estimation error bounds for RC and CC, i.e., RC achieves notably smaller estimation error than CC when complex models are used.

**Effectiveness of Generation Model.** We use *entropy* to measure how well given candidate label sets match the proposed generation model. By this measure, we could know ahead of model training whether to apply our proposed methods or not on a specific dataset. We expect that the higher the entropy, the better the match, thus the better the performance of our proposed methods. To verify our conjecture, we generate various candidate labels sets by different generation models, and the experimental results agree with our conjecture. We further show via experiments that even when given candidate label sets do not match our proposed generation model well, our methods still significantly outperform other compared methods. These experimental results are provided in Appendix F.

## 6 Conclusion

In this paper, we for the first time provided an explicit mathematical formulation of the partially labeled data generation process for PLL. Based on our data generation model, we further derived a novel *risk-consistent* method and a novel *classifier-consistent* method. To the best of our knowledge, we provided the first risk-consistent PLL method. Besides, our proposed methods do not rely on specific models and can be easily trained with stochastic optimization, which ensures their scalability to large-scale datasets. In addition, we theoretically derived an *estimation error bound* for each of the proposed methods. Finally, extensive experimental results clearly demonstrated the effectiveness of the proposed generation model and two PLL methods.

## Acknowledgements

BH was supported by the Early Career Scheme (ECS) through the Research Grants Council of Hong Kong under Grant No.22200720, HKBU Tier-1 Start-up Grant, and HKBU CSD Start-up Grant. GN and MS were supported by JST AIP Acceleration Research Grant Number JPMJCR20U3, Japan.

## References

- [1] Z.-H. Zhou, “A brief introduction to weakly supervised learning,” *National Science Review*, vol. 5, no. 1, pp. 44–53, 2018.
- [2] O. Chapelle, B. Scholkopf, and A. Zien, *Semi-Supervised Learning*. MIT Press, 2006.
- [3] G. Niu, W. Jitkrittum, B. Dai, H. Hachiya, and M. Sugiyama, “Squared-loss mutual information regularization: A novel information-theoretic approach to semi-supervised learning,” in *ICML*, pp. 10–18, 2013.
- [4] Y.-F. Li and D.-M. Liang, “Safe semi-supervised learning: a brief introduction,” *Frontiers of Computer Science*, vol. 13, no. 4, pp. 669–676, 2019.
- [5] J. Amores, “Multiple instance classification: Review, taxonomy and comparative study,” *Artificial Intelligence*, vol. 201, pp. 81–105, 2013.
- [6] Z.-H. Zhou, M.-L. Zhang, S.-J. Huang, and Y.-F. Li, “Multi-instance multi-label learning,” *Artificial Intelligence*, vol. 176, no. 1, pp. 2291–2320, 2012.
- [7] M. C. du Plessis, G. Niu, and M. Sugiyama, “Convex formulation for learning from positive and unlabeled data,” in *ICML*, pp. 1386–1394, 2015.
- [8] R. Kiryo, G. Niu, M. C. du Plessis, and M. Sugiyama, “Positive-unlabeled learning with non-negative risk estimator,” in *NeurIPS*, pp. 1674–1684, 2017.
- [9] T. Ishida, G. Niu, W. Hu, and M. Sugiyama, “Learning from complementary labels,” in *NeurIPS*, pp. 5644–5654, 2017.
- [10] T. Ishida, G. Niu, A. K. Menon, and M. Sugiyama, “Complementary-label learning for arbitrary losses and models,” in *ICML*, pp. 2971–2980, 2019.
- [11] B. Han, Q. Yao, X. Yu, G. Niu, M. Xu, W. Hu, I. Tsang, and M. Sugiyama, “Co-teaching: Robust training of deep neural networks with extremely noisy labels,” in *NeurIPS*, pp. 8527–8537, 2018.
- [12] L. Feng, S. Shu, Z. Lin, F. Lv, L. Li, and B. An, “Can cross entropy loss be robust to label noise?,” in *IJCAI*, pp. 2206–2212, 2020.
- [13] H. Wei, L. Feng, X. Chen, and B. An, “Combating noisy labels by agreement: A joint training method with co-regularization,” in *CVPR*, pp. 13726–13735, 2020.
- [14] T. Ishida, G. Niu, and M. Sugiyama, “Binary classification for positive-confidence data,” in *NeurIPS*, pp. 5917–5928, 2018.
- [15] H. Bao, G. Niu, and M. Sugiyama, “Classification from pairwise similarity and unlabeled data,” in *ICML*, pp. 452–461, 2018.
- [16] N. Lu, G. Niu, A. K. Menon, and M. Sugiyama, “On the minimal supervision for training any binary classifier from only unlabeled data,” in *ICLR*, 2019.
- [17] N. Lu, T. Zhang, G. Niu, and M. Sugiyama, “Mitigating overfitting in supervised classification from two unlabeled datasets: A consistent risk correction approach,” in *AISTATS*, 2020.
- [18] R. Jin and Z. Ghahramani, “Learning with multiple labels,” in *NeurIPS*, pp. 921–928, 2003.

- [19] T. Cour, B. Sapp, and B. Taskar, “Learning from partial labels,” *JMLR*, vol. 12, no. 5, pp. 1501–1536, 2011.
- [20] L. Liu and T. Dietterich, “Learnability of the superset label learning problem,” in *ICML*, pp. 1629–1637, 2014.
- [21] Y.-C. Chen, V. M. Patel, R. Chellappa, and P. J. Phillips, “Ambiguously labeled learning using dictionaries,” *TIFS*, vol. 9, no. 12, pp. 2076–2088, 2014.
- [22] M.-L. Zhang and F. Yu, “Solving the partial label learning problem: An instance-based approach,” in *IJCAI*, pp. 4048–4054, 2015.
- [23] L. Feng and B. An, “Partial label learning with self-guided retraining,” in *AAAI*, pp. 3542–3549, 2019.
- [24] G. Lyu, S. Feng, T. Wang, C. Lang, and Y. Li, “Gm-pll: Graph matching based partial label learning,” *TKDE*, 2019.
- [25] E. Hüllermeier and J. Beringer, “Learning from ambiguously labeled examples,” *Intelligent Data Analysis*, vol. 10, no. 5, pp. 419–439, 2006.
- [26] Z.-N. Zeng, S.-J. Xiao, K. Jia, T.-H. Chan, S.-H. Gao, D. Xu, and Y. Ma, “Learning by associating ambiguously labeled images,” in *CVPR*, pp. 708–715, 2013.
- [27] C.-H. Chen, V. M. Patel, and R. Chellappa, “Learning from ambiguously labeled face images,” *TPAMI*, vol. 40, no. 7, pp. 1653–1667, 2018.
- [28] Y. Yao, C. Gong, J. Deng, X. Chen, J. Wu, and J. Yang, “Deep discriminative cnn with temporal ensembling for ambiguously-labeled image classification,” in *AAAI*, p. in press, 2020.
- [29] L.-P. Liu and T. G. Dietterich, “A conditional multinomial mixture model for superset label learning,” in *NeurIPS*, pp. 548–556, 2012.
- [30] C. Gong, T. Liu, Y. Tang, J. Yang, J. Yang, and D. Tao, “A regularization approach for instance-based superset label learning,” *IEEE Transactions on Cybernetics*, vol. 48, no. 3, pp. 967–978, 2018.
- [31] J. Luo and F. Orabona, “Learning from candidate labeling sets,” in *NeurIPS*, pp. 1504–1512, 2010.
- [32] N. Nguyen and R. Caruana, “Classification with partial labels,” in *KDD*, pp. 551–559, 2008.
- [33] L. Feng and B. An, “Leveraging latent label distributions for partial label learning,” in *IJCAI*, pp. 2107–2113, 2018.
- [34] X. Xia, T. Liu, N. Wang, B. Han, C. Gong, G. Niu, and M. Sugiyama, “Are anchor points really indispensable in label-noise learning?,” in *NeurIPS*, pp. 6835–6846, 2019.
- [35] M.-L. Zhang, F. Yu, and C.-Z. Tang, “Disambiguation-free partial label learning,” *TKDE*, vol. 29, no. 10, pp. 2155–2167, 2017.
- [36] X. Yu, T. Liu, M. Gong, and D. Tao, “Learning with biased complementary labels,” in *ECCV*, pp. 68–83, 2018.
- [37] L. Feng, T. Kaneko, B. Han, G. Niu, B. An, and M. Sugiyama, “Learning with multiple complementary labels,” in *ICML*, 2020.

- [38] B. Han, J. Yao, G. Niu, M. Zhou, I. Tsang, Y. Zhang, and M. Sugiyama, “Masking: A new perspective of noisy supervision,” in *NeurIPS*, pp. 5836–5846, 2018.
- [39] A. Gretton, A. Smola, J. Huang, M. Schmittfull, K. Borgwardt, and B. Schölkopf, “Covariate shift by kernel mean matching,” *Dataset Shift in Machine Learning*, vol. 3, no. 4, p. 5, 2009.
- [40] P. L. Bartlett and S. Mendelson, “Rademacher and gaussian complexities: Risk bounds and structural results,” *JMLR*, vol. 3, no. 11, pp. 463–482, 2002.
- [41] N. Golowich, A. Rakhlin, and O. Shamir, “Size-independent sample complexity of neural networks,” *arXiv preprint arXiv:1712.06541*, 2017.
- [42] J. Lv, M. Xu, L. Feng, G. Niu, X. Geng, and M. Sugiyama, “Progressive identification of true labels for partial-label learning,” in *ICML*, 2020.
- [43] Y. LeCun, L. Bottou, Y. Bengio, P. Haffner, *et al.*, “Gradient-based learning applied to document recognition,” *Proceedings of the IEEE*, vol. 86, no. 11, pp. 2278–2324, 1998.
- [44] T. Clanuwat, M. Bober-Irizar, A. Kitamoto, A. Lamb, K. Yamamoto, and D. Ha, “Deep learning for classical japanese literature,” *arXiv preprint arXiv:1812.01718*, 2018.
- [45] H. Xiao, K. Rasul, and R. Vollgraf, “Fashion-mnist: A novel image dataset for benchmarking machine learning algorithms,” *arXiv preprint arXiv:1708.07747*, 2017.
- [46] A. Krizhevsky, G. Hinton, *et al.*, “Learning multiple layers of features from tiny images,” tech. rep., Citeseer, 2009.
- [47] F. Briggs, X. Z. Fern, and R. Raich, “Rank-loss support instance machines for miml instance annotation,” in *KDD*, pp. 534–542, 2012.
- [48] M. Guillaumin, J. Verbeek, and C. Schmid, “Multiple instance metric learning from automatically labeled bags of faces,” *Lecture Notes in Computer Science*, vol. 63, no. 11, pp. 634–647, 2010.
- [49] K. He, X. Zhang, S. Ren, and J. Sun, “Deep residual learning for image recognition,” in *CVPR*, pp. 770–778, 2016.
- [50] G. Huang, Z. Liu, L. Van Der Maaten, and K. Q. Weinberger, “Densely connected convolutional networks,” in *CVPR*, pp. 4700–4708, 2017.
- [51] C. Elkan and K. Noto, “Learning classifiers from only positive and unlabeled data,” in *KDD*, pp. 213–220, 2008.
- [52] A. Paszke, S. Gross, F. Massa, A. Lerer, J. Bradbury, G. Chanan, T. Killeen, Z. Lin, N. Gimeshein, L. Antiga, *et al.*, “Pytorch: An imperative style, high-performance deep learning library,” in *NeurIPS*, pp. 8024–8035, 2019.
- [53] D. P. Kingma and J. Ba, “Adam: A method for stochastic optimization,” in *ICLR*, 2015.
- [54] M. Mohri, A. Rostamizadeh, and A. Talwalkar, *Foundations of Machine Learning*. MIT Press, 2012.
- [55] C. McDiarmid, “On the method of bounded differences,” in *Surveys in Combinatorics*, 1989.
- [56] M. Ledoux and M. Talagrand, *Probability in Banach Spaces: Isoperimetry and Processes*. Springer Science & Business Media, 2013.

- [57] G. Panis and A. Lanitis, “An overview of research activities in facial age estimation using the fg-net aging database,” in *ECCV*, pp. 737–750, 2014.
- [58] N. Halko, P.-G. Martinsson, and J. A. Tropp, “Finding structure with randomness: Stochastic algorithms for constructing approximate matrix decompositions,” 2009.
- [59] D. Zhou, O. Bousquet, T. N. Lal, J. Weston, and B. Schölkopf, “Learning with local and global consistency,” in *NeurIPS*, pp. 321–328, 2004.

## A Proofs of Data Generation Process

### A.1 Proof of Theorem 1

From our formulation of the partially labeled data distribution  $\tilde{p}(\mathbf{x}, Y)$ , we can obtain the simplified expression  $\tilde{p}(\mathbf{x}, Y) = \frac{1}{2^{k-1}-1} \sum_{y \in Y} p(\mathbf{x}, y)$ . Then, we have

$$\begin{aligned}
 \int_{\mathcal{C}} \int_{\mathcal{X}} \tilde{p}(\mathbf{x}, Y) d\mathbf{x} dY &= \int_{\mathcal{X}} \sum_{Y \in \mathcal{C}} \tilde{p}(\mathbf{x}, Y) d\mathbf{x} \\
 &= \frac{1}{2^{k-1}-1} \int_{\mathcal{X}} \sum_{Y \in \mathcal{C}} \sum_{y \in Y} p(\mathbf{x}, y) d\mathbf{x} \\
 &= \frac{1}{2^{k-1}-1} \int_{\mathcal{X}} \sum_{y=1}^k \sum_{Y \in \{Y | Y \in \mathcal{C}, y \in Y\}} p(\mathbf{x}, y) d\mathbf{x} \\
 &= \frac{1}{2^{k-1}-1} \int_{\mathcal{X}} \sum_{y=1}^k (2^{k-1}-1) p(\mathbf{x}, y) d\mathbf{x} \\
 &= 1,
 \end{aligned}$$

which concludes the proof of Theorem 1. □

### A.2 Proof of Theorem 2

It is intuitive to express  $p(y \in Y | \mathbf{x}, Y)$  as

$$\begin{aligned}
 p(y \in Y | \mathbf{x}, Y) &= 1 - p(y \notin Y | \mathbf{x}, Y) \\
 &= 1 - \sum_{i \notin Y} p(y = i | \mathbf{x}, Y) \\
 &= 1 - \sum_{i \notin Y} \frac{p(Y | y = i, \mathbf{x}) p(y = i | \mathbf{x})}{p(Y | \mathbf{x})} \\
 &= 1 - \sum_{i \notin Y} \frac{p(Y | y = i) p(y = i | \mathbf{x})}{\sum_{j=1}^k p(Y | y = j) p(y = j | \mathbf{x})} \\
 &= 1 - (2^{k-1} - 1) \sum_{i \notin Y} \frac{p(Y | y = i) p(y = i | \mathbf{x})}{\sum_{j \in Y} p(y = j | \mathbf{x})} \\
 &= 1,
 \end{aligned}$$

where the last equality holds because  $p(Y | y = i) = 0$  if  $i \notin Y$ , in terms of Eq. (5). □

### A.3 Proof of Lemma 1

Let us first consider the case where the correct label  $y$  is a specific label  $i$  ( $i \in [k]$ ), then we have

$$\begin{aligned}
p(y \in Y, y = i | \mathbf{x}) &= p(y \in Y | y = i, \mathbf{x})p(y = i | \mathbf{x}) \\
&= \sum_{C \in \mathcal{C}} p(y \in Y, Y = C | y = i, \mathbf{x})p(y = i | \mathbf{x}) \\
&= \sum_{C \in \mathcal{C}} p(y \in Y | Y = C, y = i, \mathbf{x})p(y = i | \mathbf{x})p(Y = C | \mathbf{x}) \\
&= \sum_{C \in \mathcal{C}} p(y \in Y | Y = C, y = i, \mathbf{x})p(y = i | \mathbf{x})p(Y = C) \\
&= \frac{1}{2^k - 2} \sum_{C \in \mathcal{C}} p(y \in Y | Y = C, y = i, \mathbf{x})p(y = i | \mathbf{x}) \\
&= \frac{1}{2^k - 2} |\mathcal{C}^i| \cdot p(y = i | \mathbf{x}) \\
&= \frac{2^{k-1} - 1}{2^k - 2} p(y = i | \mathbf{x}) \\
&= \frac{1}{2} p(y = i | \mathbf{x}),
\end{aligned}$$

where we have used  $p(Y = C | \mathbf{x}) = p(Y = C) = \frac{1}{2^k - 2}$  because  $Y$  is sampled from the whole set of label sets uniformly at random. In addition,  $\mathcal{C}^i = \{Y \in \mathcal{C} | i \in Y\}$  denotes the set of all the label sets that contain  $i$ , hence we can obtain  $|\mathcal{C}^i| = 2^{k-1} - 1$ . By further summing up the both side over all possible  $i$ , we can obtain

$$\sum_i p(y \in Y, y = i | \mathbf{x}) = \sum_i \frac{1}{2} p(y = i | \mathbf{x}) \Rightarrow p(y \in Y | \mathbf{x}) = \frac{1}{2},$$

which concludes the proof of Lemma 1. □

### A.4 Proof of Theorem 3

Let us express  $p(Y | y \in Y, \mathbf{x})$  as

$$\begin{aligned}
p(Y | y \in Y, \mathbf{x}) &= \frac{p(y \in Y, Y | \mathbf{x})}{p(y \in Y | \mathbf{x})} \\
&= \frac{p(y \in Y | Y, \mathbf{x})p(Y | \mathbf{x})}{p(y \in Y | \mathbf{x})} \\
&= \frac{p(y \in Y | Y, \mathbf{x})p(Y)}{p(y \in Y | \mathbf{x})} \\
&= \frac{2}{2^k - 2} p(y \in Y | Y, \mathbf{x}) \quad (\because p(y \in Y | \mathbf{x}) = \frac{1}{2} \text{ and } p(Y) = \frac{1}{2^k - 2}) \\
&= \frac{1}{2^{k-1} - 1} \sum_{y \in Y} p(y | \mathbf{x}).
\end{aligned}$$

By further multiplying  $p(\mathbf{x})$  on both side, we can obtain  $p(\mathbf{x}, Y | y \in Y) = \frac{1}{2^{k-1} - 1} \sum_{y \in Y} p(\mathbf{x}, y) = \tilde{p}(\mathbf{x}, Y)$  where  $\tilde{p}(\mathbf{x}, Y)$  is our presented data distribution for PLL. □

## B Proofs of Theorem 4

Our proof of the estimation error bound is based on *Rademacher complexity* [40].

**Definition 7** (Rademacher complexity). *Let  $Z_1, \dots, Z_n$  be  $n$  i.i.d. random variables drawn from a probability distribution  $\mu$ ,  $\mathcal{H} = \{h : \mathcal{Z} \rightarrow \mathbb{R}\}$  be a class of measurable functions. Then the expected Rademacher complexity of  $\mathcal{H}$  is defined as*

$$\mathfrak{R}_n(\mathcal{H}) = \mathbb{E}_{Z_1, \dots, Z_n \sim \mu} \mathbb{E}_{\boldsymbol{\sigma}} \left[ \sup_{h \in \mathcal{H}} \frac{1}{n} \sum_{i=1}^n \sigma_i h(Z_i) \right],$$

where  $\boldsymbol{\sigma} = (\sigma_1, \dots, \sigma_n)$  are Rademacher variables taking the value from  $\{-1, +1\}$  with even probabilities.

Before proving Theorem 4, we introduce the following lemma.

**Lemma 4.** *Let  $\hat{f}$  be the empirical risk minimizer (i.e.,  $\hat{f} = \arg \min_{f \in \mathcal{F}} \hat{R}(f)$ ) and  $f^*$  be the true risk minimizer (i.e.,  $f^* = \arg \min_{f \in \mathcal{F}} R(f)$ ), then the following inequality holds:*

$$R(\hat{f}) - R(f^*) \leq 2 \sup_{f \in \mathcal{F}} |\hat{R}(f) - R(f)|.$$

*Proof.* It is intuitive to obtain

$$\begin{aligned} R(\hat{f}) - R(f^*) &\leq R(\hat{f}) - \hat{R}(\hat{f}) + \hat{R}(\hat{f}) - R(f^*) \\ &\leq R(\hat{f}) - \hat{R}(\hat{f}) + R(\hat{f}) - R(f^*) \\ &\leq 2 \sup_{f \in \mathcal{F}} |\hat{R}(f) - R(f)|, \end{aligned}$$

which completes the proof. The same proof has been provided in [54]. □

Then, we define a function space for our RC method as

$$\mathcal{G}_{\text{rc}} = \{(\mathbf{x}, Y) \mapsto \frac{1}{2} \sum_{i=1}^k \frac{p(y=i | \mathbf{x})}{\sum_{j \in Y} p(y=j | \mathbf{x})} \mathcal{L}(f(\mathbf{x}), i) \mid f \in \mathcal{F}\},$$

where  $(\mathbf{x}, Y)$  is randomly sampled from  $\tilde{p}(\mathbf{x}, Y)$ . Let  $\tilde{\mathfrak{R}}_n(\mathcal{G}_{\text{rc}})$  be the expected Rademacher complexity of  $\mathcal{G}_{\text{rc}}$ , i.e.,

$$\tilde{\mathfrak{R}}_n(\mathcal{G}_{\text{rc}}) = \mathbb{E}_{\tilde{p}(\mathbf{x}, Y)} \mathbb{E}_{\boldsymbol{\sigma}} \left[ \sup_{g \in \mathcal{G}_{\text{rc}}} \frac{1}{n} \sum_{i=1}^n \sigma_i g(\mathbf{x}_i, Y_i) \right].$$

Then we have the following lemma.

**Lemma 5.** *Suppose the loss function  $\mathcal{L}$  is bounded by  $M$ , i.e.,  $M = \sup_{\mathbf{x} \in \mathcal{X}, f \in \mathcal{F}, y \in \mathcal{Y}} \mathcal{L}(f(\mathbf{x}), y)$ , then for any  $\delta > 0$ , with probability at least  $1 - \delta$ ,*

$$\sup_{f \in \mathcal{F}} |R_{\text{rc}}(f) - \hat{R}_{\text{rc}}(f)| \leq 2\tilde{\mathfrak{R}}_n(\mathcal{G}_{\text{rc}}) + \frac{M}{2} \sqrt{\frac{\log \frac{2}{\delta}}{2n}}.$$

*Proof.* In order to prove this lemma, we first show that the one direction  $\sup_{f \in \mathcal{F}} R_{\text{rc}}(f) - \widehat{R}_{\text{rc}}(f)$  is bounded with probability at least  $1 - \delta/2$ , and the other direction can be similarly shown. Suppose an example  $(\mathbf{x}_i, Y_i)$  is replaced by another arbitrary example  $(\mathbf{x}'_i, Y'_i)$ , then the change of  $\sup_{f \in \mathcal{F}} R_{\text{rc}}(f) - \widehat{R}_{\text{rc}}(f)$  is no greater than  $M/(2n)$ , since  $\mathcal{L}$  is bounded by  $M$ . By applying *McDiarmid's inequality* [55], for any  $\delta > 0$ , with probability at least  $1 - \delta/2$ ,

$$\sup_{f \in \mathcal{F}} R_{\text{rc}}(f) - \widehat{R}_{\text{rc}}(f) \leq \mathbb{E} \left[ \sup_{f \in \mathcal{F}} R_{\text{rc}}(f) - \widehat{R}_{\text{rc}}(f) \right] + \frac{M}{2} \sqrt{\frac{\log \frac{2}{\delta}}{2n}}.$$

Using the same trick in [54], we can obtain

$$\mathbb{E} \left[ \sup_{f \in \mathcal{F}} R_{\text{rc}}(f) - \widehat{R}_{\text{rc}}(f) \right] \leq 2\widetilde{\mathfrak{R}}_n(\mathcal{G}_{\text{rc}}).$$

By further taking into account the other side  $\sup_{f \in \mathcal{F}} \widehat{R}_{\text{rc}}(f) - R_{\text{rc}}(f)$ , we have for any  $\delta > 0$ , with probability at least  $1 - \delta$ ,

$$\sup_{f \in \mathcal{F}} \left| R_{\text{rc}}(f) - \widehat{R}_{\text{rc}}(f) \right| \leq 2\widetilde{\mathfrak{R}}_n(\mathcal{G}_{\text{rc}}) + \frac{M}{2} \sqrt{\frac{\log \frac{2}{\delta}}{2n}},$$

which concludes the proof.  $\square$

Next, we will bound the expected Rademacher complexity of  $\mathcal{G}_{\text{rc}}$  (i.e.,  $\widetilde{\mathfrak{R}}_n(\mathcal{G}_{\text{rc}})$ ) by the following lemma.

**Lemma 6.** *Assume the loss function  $\mathcal{L}(f(\mathbf{x}), y)$  is  $\rho$ -Lipschitz with respect to  $f_y(\mathbf{x})$  ( $0 < \rho < \infty$ ) for all  $y \in \mathcal{Y}$ . Then, the following inequality holds:*

$$\widetilde{\mathfrak{R}}_n(\mathcal{G}_{\text{rc}}) \leq \rho \sum_{y=1}^k \mathfrak{R}_n(\mathcal{H}_y),$$

where

$$\begin{aligned} \mathcal{H}_y &= \{h : \mathbf{x} \mapsto f_y(\mathbf{x}) \mid f \in \mathcal{F}\}, \\ \mathfrak{R}_n(\mathcal{H}_y) &= \mathbb{E}_{p(\mathbf{x})} \mathbb{E}_{\sigma} \left[ \sup_{h \in \mathcal{H}_y} \frac{1}{n} \sum_{i=1}^n h(\mathbf{x}_i) \right]. \end{aligned}$$

*Proof.* The expected Rademacher complexity of  $\tilde{\mathfrak{R}}_n(\mathcal{G}_{\text{rc}})$  can be expressed as

$$\begin{aligned}
\tilde{\mathfrak{R}}_n(\mathcal{G}_{\text{rc}}) &= \mathbb{E}_{\tilde{p}(\mathbf{x}, Y)} \mathbb{E}_{\sigma} \left[ \sup_{g \in \mathcal{G}_{\text{rc}}} \frac{1}{n} \sum_{i=1}^n \sigma_i g(\mathbf{x}_i, Y_i) \right] \\
&= \mathbb{E}_{\tilde{p}(\mathbf{x}, Y)} \mathbb{E}_{\sigma} \left[ \sup_{f \in \mathcal{F}} \frac{1}{n} \sum_{i=1}^n \sigma_i \left( \sum_{l=1}^k \frac{p(y=l | \mathbf{x}_i)}{\sum_{j \in Y_i} p(y=j | \mathbf{x}_i)} \mathcal{L}(f(\mathbf{x}_i), l) \right) \right] \\
&\leq \mathbb{E}_{\tilde{p}(\mathbf{x}, Y)} \mathbb{E}_{\sigma} \left[ \sup_{f \in \mathcal{F}} \frac{1}{n} \sum_{i=1}^n \left( \sum_{y=1}^k \sigma_i \mathcal{L}(f(\mathbf{x}_i), y) \right) \right] \\
&\leq \sum_{y=1}^k \mathbb{E}_{\tilde{p}(\mathbf{x}, Y)} \mathbb{E}_{\sigma} \left[ \sup_{f \in \mathcal{F}} \frac{1}{n} \sum_{i=1}^n \left( \sigma_i \mathcal{L}(f(\mathbf{x}_i), y) \right) \right] \\
&\leq \sum_{y=1}^k \mathbb{E}_{p(\mathbf{x})} \mathbb{E}_{\sigma} \left[ \sup_{f \in \mathcal{F}} \frac{1}{n} \sum_{i=1}^n \left( \sigma_i \mathcal{L}(f(\mathbf{x}_i), y) \right) \right] \\
&= (\star),
\end{aligned}$$

where the first inequality holds due to  $\frac{p(y=l|\mathbf{x}_i)}{\sum_{j \in Y_i} p(y=j|\mathbf{x}_i)} \leq 1, \forall l \in [k], \forall (\mathbf{x}_i, Y_i) \sim \tilde{p}(\mathbf{x}, Y)$ . Since  $\mathcal{L}(f(\mathbf{x}_i), y)$  is  $\rho$ -Lipschitz w.r.t.  $f_y(\mathbf{x}_i), \forall y \in \mathcal{Y}$ , by further applying the *Talagrand Contraction Lemma* [56], we have

$$\begin{aligned}
(\star) &= \sum_{y=1}^k \mathbb{E}_{p(\mathbf{x})} \mathbb{E}_{\sigma} \left[ \sup_{f \in \mathcal{F}} \frac{1}{n} \sum_{i=1}^n \left( \sigma_i \mathcal{L}(f(\mathbf{x}_i), y) \right) \right] \\
&\leq \rho \sum_{y=1}^k \mathbb{E}_{p(\mathbf{x})} \mathbb{E}_{\sigma} \left[ \sup_{f \in \mathcal{F}} \frac{1}{n} \sum_{i=1}^n \left( \sigma_i f_y(\mathbf{x}_i) \right) \right] \\
&= \rho \sum_{y=1}^k \mathbb{E}_{p(\mathbf{x})} \mathbb{E}_{\sigma} \left[ \sup_{h \in \mathcal{H}_y} \frac{1}{n} \sum_{i=1}^n \left( \sigma_i h(\mathbf{x}_i) \right) \right] \\
&= \rho \sum_{y=1}^k \mathfrak{R}_n(\mathcal{H}_y),
\end{aligned}$$

which concludes the proof. □

Combining Lemma 4, Lemma 5, and Lemma 6, Theorem 4 is proved. □

## C Proofs of Classifier-Consistency

### C.1 Proof of Lemma 2

To prove that  $\mathbf{Q}$  is invertible, we resort to the definition of  $\mathbf{Q}$ , which relies on the equality  $p(Y | \mathbf{x}) = \sum_{y \in Y} \frac{1}{2^k - 1} p(y | \mathbf{x})$ . We start by defining  $\mathcal{C}^y$  as the set of all the possible label sets that include a specific label  $y \in \mathcal{Y}$ , i.e.,

$$\mathcal{C}^y := \{Y \in \mathcal{C} \mid y \in Y\}.$$

Then we can obtain

$$\begin{aligned}
\sum_{Y \in \mathcal{C}^y} p(Y | \mathbf{x}) &= \frac{1}{2^{k-1} - 1} \sum_{Y \in \mathcal{C}^y} \sum_{y \in Y} p(y | \mathbf{x}) \\
&= \frac{1}{2^{k-1} - 1} \sum_{y'} \sum_{Y' \in \{Y' \in \mathcal{C}^y | y' \in Y'\}} p(y' | \mathbf{x}) \\
&= \frac{2^{k-1} - 1}{2^{k-1} - 1} p(y | \mathbf{x}) + \frac{2^{k-2}}{2^{k-1} - 1} \sum_{y' \neq y} p(y' | \mathbf{x}) \\
&= p(y | \mathbf{x}) + \frac{2^{k-2}}{2^{k-1} - 1} (1 - p(y | \mathbf{x})) \\
&= \frac{2^{k-2} - 1}{2^{k-1} - 1} p(y | \mathbf{x}) + \frac{2^{k-2}}{2^{k-1} - 1}.
\end{aligned}$$

By multiplying both sides by  $(2^{k-1} - 1)$ , we have

$$\begin{aligned}
(2^{k-1} - 1) \sum_{Y \in \mathcal{C}^y} p(Y | \mathbf{x}) &= (2^{k-2} - 1)p(y | \mathbf{x}) + 2^{k-2} \\
\frac{2^{k-1} - 1}{2^{k-2} - 1} \sum_{Y \in \mathcal{C}^y} p(Y | \mathbf{x}) &= p(y | \mathbf{x}) + \frac{2^{k-2}}{2^{k-2} - 1} \\
p(y | \mathbf{x}) &= \frac{2^{k-1} - 1}{2^{k-2} - 1} \sum_{Y \in \mathcal{C}^y} p(Y | \mathbf{x}) - \frac{2^{k-2}}{2^{k-2} - 1}.
\end{aligned}$$

We recall that  $g_i(\mathbf{x}) = p(y = i | \mathbf{x})$  ( $i \in [k]$ ),  $q_j(\mathbf{x}) = p(Y = C_j | \mathbf{x})$  ( $j \in [2^k - 2]$ ), and define the matrix  $\mathbf{A} \in \mathbb{R}^{k \times (2^k - 2)}$  as

$$\begin{bmatrix}
p(y = 1 | Y = C_1) & \cdots & p(y = 1 | Y = C_{2^{k-2}}) \\
p(y = 2 | Y = C_1) & \cdots & p(y = 2 | Y = C_{2^{k-2}}) \\
\vdots & \ddots & \vdots \\
p(y = k | Y = C_1) & \cdots & p(y = k | Y = C_{2^{k-2}})
\end{bmatrix},$$

where  $A_{ij} = p(y = i | Y = C_j) = \frac{2^{k-1} - 1}{2^{k-2} - 1}$  if  $Y \in \mathcal{C}^y$  otherwise 0. With these notations, we can obtain

$$\begin{aligned}
g(\mathbf{x}) &= \mathbf{A}q(\mathbf{x}) - \frac{2^{k-2}}{2^{k-2} - 1} \mathbf{1}q(\mathbf{x}) \\
&= (\mathbf{A} - \frac{2^{k-2}}{2^{k-2} - 1} \mathbf{1})q(\mathbf{x}),
\end{aligned}$$

where  $\mathbf{1} = [1]^{k \times (2^k - 2)}$ . Recall that  $q(\mathbf{x}) = \mathbf{Q}^\top g(\mathbf{x})$ , hence  $g(\mathbf{x}) = \mathbf{Q}^{-\top} q(\mathbf{x})$ . Which means,  $\mathbf{Q}^{-\top} = \mathbf{A} - \frac{2^{k-2}}{2^{k-2} - 1} \mathbf{1}$ . In this way, we have proved that  $\mathbf{Q}$  is invertible.  $\square$

## C.2 Proof of Lemma 3

**Cross Entropy Loss** If the cross entropy loss is used, we have the following optimization problem:

$$\begin{aligned}\phi(g) &= - \sum_{i=1}^k p(y = i | \mathbf{x}) \log(g_i(\mathbf{x})) \\ \text{s.t. } & \sum_{i=1}^k g_i(\mathbf{x}) = 1.\end{aligned}$$

By using the Lagrange multiplier method, we can obtain the following non-constrained optimization problem:

$$\Phi(g) = - \sum_{i=1}^k p(y = i | \mathbf{x}) \log(g_i(\mathbf{x})) + \lambda \left( \sum_{i=1}^k g_i(\mathbf{x}) - 1 \right).$$

By setting the derivative to 0, we obtain

$$g_i^*(\mathbf{x}) = \frac{1}{\lambda} p(y = i | \mathbf{x}).$$

Because  $\sum_{i=1}^k g_i^*(\mathbf{x}) = 1$  and  $\sum_{i=1}^k p(y = i | \mathbf{x}) = 1$ , we have

$$\sum_{i=1}^k g_i^*(\mathbf{x}) = \frac{1}{\lambda} \sum_{i=1}^k p(y = i | \mathbf{x}) = 1.$$

Therefore, we can easily obtain  $\lambda = 1$ . In this way,  $g_i^* = \frac{1}{\lambda} p(y = i | \mathbf{x}) = p(y = i | \mathbf{x})$ , which concludes the proof.

**Mean Squared Error** If the mean squared error is used, we have the following optimization problem:

$$\begin{aligned}\phi(g) &= \sum_{i=1}^k (p(y = i | \mathbf{x}) - g_i(\mathbf{x}))^2 \\ \text{s.t. } & \sum_{i=1}^k g_i(\mathbf{x}) = 1.\end{aligned}$$

By using the Lagrange multiplier method, we can obtain the following non-constrained optimization problem:

$$\Phi(g) = \sum_{i=1}^k (p(y = i | \mathbf{x}) - g_i(\mathbf{x}))^2 + \lambda' \left( \sum_{i=1}^k g_i(\mathbf{x}) - 1 \right).$$

By setting the derivative to 0, we obtain

$$g_i^*(\mathbf{x}) = p(y = i | \mathbf{x}) - \frac{\lambda'}{2}.$$

Because  $\sum_{i=1}^k g_i^*(\mathbf{x}) = 1$  and  $\sum_{i=1}^k p(y = i | \mathbf{x}) = 1$ , we have

$$\begin{aligned}\sum_{i=1}^k g_i^*(\mathbf{x}) &= \sum_{i=1}^k p(y = i | \mathbf{x}) - \frac{\lambda' k}{2} \\ 0 &= -\frac{\lambda' k}{2}.\end{aligned}$$

Since  $k \neq 0$ , we can obtain  $\lambda' = 0$ . In this way,  $g_i^* = p(y = i | \mathbf{x}) - \frac{\lambda'}{2} = p(y = i | \mathbf{x})$ , which concludes the proof.

### C.3 Proof of Theorem 5

When minimizing  $R_{\text{cc}}(f)$ , we can approximately obtain

$$q_j^*(\mathbf{x}) = p(Y = C_j | \mathbf{x}).$$

Let  $\tilde{\mathbf{v}} = [p(Y = C_1 | \mathbf{x}), p(Y = C_2 | \mathbf{x}), \dots, p(Y = C_{2^k-2} | \mathbf{x})]$  and  $\mathbf{v} = [p(y = 1 | \mathbf{x}), p(y = 2 | \mathbf{x}), \dots, p(y = k | \mathbf{x})]$ . According to the equality  $q(\mathbf{x}) = \mathbf{Q}^\top g(\mathbf{x})$ , we have

$$\tilde{\mathbf{v}} = \mathbf{Q}^\top \mathbf{v},$$

which further ensures

$$q^*(\mathbf{x}) = \tilde{\mathbf{v}} = \mathbf{Q}^\top \mathbf{v} = \mathbf{Q}^\top g^*(\mathbf{x}).$$

Therefore, if the transition matrix  $\mathbf{Q}$  is invertible, we can find the optimal  $g^*(\mathbf{x}) = \mathbf{v}$ , which implies  $f^* = f_{\text{cc}}$ .  $\square$

## D Proof of Theorem 6

Since this proof is somewhat similar to the proof of Theorem 4, we briefly sketch the key points.

We define a function space for our CC method as

$$\mathcal{G}_{\text{cc}} = \{(\mathbf{x}, Y) \mapsto \mathcal{L}(q(\mathbf{x}), \tilde{y}) \mid f \in \mathcal{F}\},$$

where  $(\mathbf{x}, Y)$  is randomly sampled from  $\tilde{p}(\mathbf{x}, Y)$  and  $C_{\tilde{y}} = Y$  (i.e.,  $Y$  is the  $\tilde{y}$ -th label set in  $\mathcal{C}$ ). Let  $\tilde{\mathfrak{R}}_n(\mathcal{G}_{\text{cc}})$  be the expected Rademacher complexity of  $\mathcal{G}_{\text{cc}}$ , i.e.,

$$\tilde{\mathfrak{R}}_n(\mathcal{G}_{\text{cc}}) = \mathbb{E}_{\tilde{p}(\mathbf{x}, Y)} \mathbb{E}_{\sigma} \left[ \sup_{g \in \mathcal{G}_{\text{cc}}} \frac{1}{n} \sum_{i=1}^n \sigma_i g(\mathbf{x}_i, Y_i) \right].$$

Then we have the following lemma.

**Lemma 7.** *Suppose the loss function  $\mathcal{L}$  is bounded by  $M$ , i.e.,  $M = \sup_{\mathbf{x} \in \mathcal{X}, f \in \mathcal{F}, \tilde{y} \in \tilde{\mathcal{Y}}} \mathcal{L}(q(\mathbf{x}), \tilde{y})$ , then for any  $\delta > 0$ , with probability at least  $1 - \delta$ ,*

$$\sup_{f \in \mathcal{F}} |R_{\text{cc}}(f) - \widehat{R}_{\text{cc}}(f)| \leq 2\tilde{\mathfrak{R}}_n(\mathcal{G}_{\text{cc}}) + \frac{M}{2} \sqrt{\frac{\log \frac{2}{\delta}}{2n}}.$$

*Proof.* In order to prove this lemma, we first show that the one direction  $\sup_{f \in \mathcal{F}} R_{\text{cc}}(f) - \widehat{R}_{\text{cc}}(f)$  is bounded with probability at least  $1 - \delta/2$ , and the other direction can be similarly shown. Suppose an example  $(\mathbf{x}_i, Y_i)$  is replaced by another arbitrary example  $(\mathbf{x}'_i, Y'_i)$ , then the change of  $\sup_{f \in \mathcal{F}} R_{\text{cc}}(f) - \widehat{R}_{\text{cc}}(f)$  is no greater than  $M/n$ , since  $\mathcal{L}$  is bounded by  $M$ . By applying *McDiarmid's inequality* [55], for any  $\delta > 0$ , with probability at least  $1 - \delta/2$ ,

$$\sup_{f \in \mathcal{F}} R_{\text{cc}}(f) - \widehat{R}_{\text{cc}}(f) \leq \mathbb{E} \left[ \sup_{f \in \mathcal{F}} R_{\text{cc}}(f) - \widehat{R}_{\text{cc}}(f) \right] + M \sqrt{\frac{\log \frac{2}{\delta}}{2n}}.$$

Table 5: Characteristics of the controlled datasets.

Dataset	#Train	#Test	#Features	#Classes	Model
Yeast	1,335	149	8	10	Linear Model
Texture	4,950	550	40	11	Linear Model
Dermatology	329	37	34	6	Linear Model
Har	9,269	1,030	561	6	Linear Model
20Newsgroups	16,961	1,885	300	20	Linear Model
MNIST	60,000	10,000	784	10	three-layer ( $d=500-10$ ) MLP, LeNet
Fashion-MNIST	60,000	10,000	784	10	three-layer ( $d=500-10$ ) MLP, LeNet
Kuzushiji-MNIST	60,000	10,000	784	10	three-layer ( $d=500-10$ ) MLP, LeNet
CIFAR-10	50,000	10,000	3,072	10	34-layer ResNet, 22-layer DenseNet

Using the same trick in [54], we can obtain  $\mathbb{E}[\sup_{f \in \mathcal{F}} R_{cc}(f) - \widehat{R}_{cc}(f)] \leq 2\widetilde{\mathfrak{R}}_n(\mathcal{G}_{cc})$ . By further taking into account the other side  $\sup_{f \in \mathcal{F}} \widehat{R}_{cc}(f) - R_{cc}(f)$ , we have for any  $\delta > 0$ , with probability at least  $1 - \delta$ ,

$$\sup_{f \in \mathcal{F}} |R_{cc}(f) - \widehat{R}_{cc}(f)| \leq 2\widetilde{\mathfrak{R}}_n(\mathcal{G}_{cc}) + M \sqrt{\frac{\log \frac{2}{\delta}}{2n}},$$

which concludes the proof.  $\square$

Suppose the loss function  $\mathcal{L}(q(\mathbf{x}), \tilde{y})$  is  $\rho'$ -Lipschitz with respect to  $f_y(\mathbf{x})$  ( $0 \leq \rho \leq \infty$ ) for all  $y \in \mathcal{Y}$  and  $\tilde{y} \in \widetilde{\mathcal{Y}}$ , following the proof of Lemma 6, we can obtain  $\widetilde{\mathfrak{R}}_n(\mathcal{G}_{cc}) \leq 2\rho' \sum_{y=1}^k \mathfrak{R}_n(\mathcal{H}_y)$ . By further taking into account Lemma 7 and Lemma 4, we have for any  $\delta > 0$ , with probability  $1 - \delta$ ,

$$R_{cc}(\widehat{f}_{cc}) - R_{cc}(f^*) = R_{cc}(\widehat{f}_{cc}) - R_{cc}(f_{cc}) \leq 8\rho' \sum_{y=1}^k \mathfrak{R}_n(\mathcal{H}_y) + 2M \sqrt{\frac{\log \frac{2}{\delta}}{2n}},$$

which concludes the proof of Theorem 6.  $\square$

## E Detailed Information of Experiments

In this section, we provide more detailed information of the experiments.

### E.1 Datasets and Models

**Benchmark Datasets.** We use four widely-used benchmark datasets (including MNIST, Kuzushiji-MNIST, Fashion-MNIST, CIFAR-10) and five datasets (including Yeast, Texture, Dermatology, Har, 20Newsgroups) from the UCI Machine Learning Repository. The statistics of these datasets with the corresponding base models are reported in Table 5. It is worth noting that we only use the linear model on the UCI datasets, since they are not large-scale datasets. We report the descriptions of these datasets with the sources as follows.

- MNIST<sup>1</sup> [43]: It is a 10-class dataset of handwritten digits (0 to 9). Each instance is a  $28 \times 28$  grayscale image.

<sup>1</sup><http://yann.lecun.com/exdb/mnist/>

Table 6: Characteristics of the real-world partially labeled datasets.

Dataset	#Examples	#Features	#Classes	Avg. #CLs	Application Domain	Model
Lost	1,122	108	16	2.23	<i>automatic face naming</i> [57]	Linear Model
MSRCv2	1,758	48	23	3.16	<i>object classification</i> [29]	Linear Model
BirdSong	4,998	38	13	2.18	<i>bird song classification</i> [47]	Linear Model
Soccer Player	17,472	279	171	2.09	<i>automatic face naming</i> [26]	Linear Model
Yahoo! News	22,991	163	219	1.91	<i>automatic face naming</i> [48]	Linear Model

- Kuzushiji-MNIST<sup>2</sup> [44]: It is a 10-class dataset of fashion items (T-shirt/top, trouser, pullover, dress, sandal, coat, shirt, sneaker, bag, and ankle boot). Each instance is a  $28 \times 28$  grayscale image.
- Fashion-MNIST<sup>3</sup> [45]: It is a 10-class dataset of cursive Japanese (“Kuzushiji”) characters. Each instance is a  $28 \times 28$  grayscale image.
- CIFAR-10<sup>4</sup> [46]: It is a 10-class dataset of 10 different objects (airplane, bird, automobile, cat, deer, dog, frog, horse, ship, and truck). Each instance is a  $32 \times 32 \times 3$  colored image in RGB format. This dataset is normalized with mean (0.4914, 0.4822, 0.4465) and standard deviation (0.247, 0.243, 0.261).
- 20Newsgroups<sup>5</sup>: It is a 20-class dataset of 20 different newsgroups (sci.crypt, sci.electronics, sci.med, sci.space, comp.graphics, comp.os.ms-windows.misc, comp.sys.ibm.pc.hardware, comp.sys.mac.hardware, comp.windows.x, rec.autos, rec.motorcycles, rec.sport.baseball, rec.sport.hockey, misc.forsale, talk.politics.misc, talk.politics.guns, talk.politics.mideast, talk.religion.misc, alt.atheism, soc.religion.christian). We obtained the tf-idf features, and applied TruncatedSVD [58] to reduce the dimension to 300. We randomly sample 90% of the examples from the whole dataset to construct the training set, and the rest 10% forms the test set.
- Yeast, Texture, Dermatology, Har<sup>6</sup>: They are all the datasets from the UCI Machine Learning Repository. Since they are all regular-scale datasets, we only apply linear model on them. For each dataset, we randomly sample 90% of the examples from the whole dataset to construct the training set, and the rest 10% forms the test set.

We run 5 trials on the four benchmark datasets and run 10 trials on the five UCI datasets, and record the mean accuracy with standard deviation. For the used models, the detailed information of the used 34-layer ResNet [49] and 22-layer DenseNet [50] can be found in the corresponding papers.

**Real-World Partially Labeled Datasets.** We also use five real-world partially labeled datasets<sup>7</sup>, including Lost, BirdSong, MSRCv2, Soccer Player, Yahoo! News. Table 6 reports the characteristics of these real-world partially labeled datasets, including Lost [19], Birdsong [47], MSRCv2 [29], Soccer Player [26], Yahoo! News [48]. These real-world partially labeled datasets come from several application domains. Specifically, Lost, Soccer Player, and Yahoo! News are from *automatic face naming*, Birdsong is from *bird song classification*, and MSRCv2 is from *object classification*. For automatic face naming, each face cropped from an image or a video frame is taken as an instance, and the names appearing on the corresponding

<sup>2</sup><https://github.com/rois-codh/kmnist>

<sup>3</sup><https://github.com/zalandoresearch/fashion-mnist>

<sup>4</sup><https://www.cs.toronto.edu/~kriz/cifar.html>

<sup>5</sup><http://qwone.com/~jason/20Newsgroups/>

<sup>6</sup><https://archive.ics.uci.edu/ml/datasets.php>

<sup>7</sup>[http://palm.seu.edu.cn/zhangml/Resources.htm#partial\\_data](http://palm.seu.edu.cn/zhangml/Resources.htm#partial_data)

Table 7: Transductive accuracy of each method using neural networks on benchmark datasets. ResNet is trained on CIFAR-10, and MLP is trained on the other three datasets.

	MNIST	Kuzushiji-MNIST	Fashion-MNIST	CIFAR-10
RC	<b>98.81±0.02%</b>	<b>97.45±0.06%</b>	<b>94.30±0.09%</b>	<b>87.48±0.44%</b>
CC	98.77±0.06%	97.31±0.05%●	93.55±0.14%●	86.15±0.26%●
GA	96.72±0.11%●	94.85±0.08%●	87.34±0.10%●	76.70±0.21%●
NN	97.25±0.08%●	93.91±0.06%●	88.83±0.18%●	74.31±0.35%●
Free	88.38±0.51%●	83.73±0.31%●	82.77±0.61%●	17.74±1.11%●
PC	93.42±0.12%●	88.26±0.10%●	85.54±0.18%●	46.93±2.35%●
Forward	98.68±0.04%●	96.89±0.07%●	91.48±0.26%●	78.72±1.32%●
EXP	98.70±0.03%	97.03±0.12%●	92.60±0.05%●	79.52±0.56%●
LOG	98.75±0.06%	97.18±0.06%●	93.52±0.06%●	85.96±0.45%
MAE	98.63±0.05%●	97.01±0.04%●	92.02±0.08%●	74.31±3.24%●
MSE	97.35±0.24%●	95.61±0.06%●	90.53±0.12%●	69.81±2.43%●
GCE	97.15±0.03%●	95.41±0.04%●	90.80±0.16%●	77.77±0.60%●
Phuber-CE	95.59±0.30%●	91.66±0.23%●	88.65±0.12%●	65.42±0.96%●

captions or subtitles are considered as candidate labels. For object classification, each image segment is regarded as an instance, and objects appearing in the same image are taken as candidate labels. For bird song classification, singing syllables of the birds are represented as instances and bird species jointly singing during a 10-seconds period are regarded as candidate labels. For each real-world partially labeled dataset, the average number of candidate labels (Avg. #CLs) per instance is also recorded in Table 6. In the experiments, we run 10 trials (with 90%/10% train/test split) on each real-world partially labeled dataset, and the mean accuracy with standard deviation is recorded for each method. Note that most of the existing parametric PLL methods adopt the linear model, hence we also apply linear model on these real-world partially labeled datasets for fair comparisons.

On all the above datasets, we take the average accuracy of the last ten epochs as the accuracy for each trial. All the experiments are conducted on NVIDIA Tesla V100 GPUs. Since our proposed methods are compatible with any stochastic optimizer, the time complexity of optimization could be in the linear order with respect to the number of data points.

## E.2 Compared Methods

The compared PLL methods are listed as follows.

- SURE [23]: It iteratively enlarges the confidence of the candidate label with the highest probability to be the correct label.
- CLPL [19]: It uses a convex formulation by using the one-versus-all strategy in the multi-class loss function.
- IPAL [22]: It is a non-parametric method that applies the label propagation strategy [59] to iteratively update the confidence of each candidate label.
- PLSVM [51]: It is a maximum margin-based method that differentiates candidate labels from non-candidate labels by maximizing the margin between them.
- PLECO [35]: It adapts the Error-Correcting Output Codes method to deal with partially labeled examples in a disambiguation-free manner.

Table 8: Transductive accuracy of each method using neural networks on benchmark datasets. DenseNet is trained on CIFAR-10, and LeNet is trained on the other three datasets.

	MNIST	Kuzushiji-MNIST	Fashion-MNIST	CIFAR-10 ResNet
RC	<b>99.46±0.02%</b>	98.69±0.03%	<b>94.32±0.07%</b>	<b>86.77±0.47%</b>
CC	99.43±0.03%	<b>98.78±0.01%</b>	94.31±0.17%	85.38±0.16%●
GA	95.58±0.02%●	97.13±0.02%●	89.33±0.03%●	75.38±0.23%●
NN	98.72±0.04%●	96.99±0.06%●	90.35±0.19%●	75.12±0.25%●
Free	79.98±2.03%●	84.01±1.36%●	75.03±3.95%●	46.65±0.35%●
PC	95.32±0.13%●	90.80±0.12%●	85.39±0.18%●	55.68±2.30%●
Forward	99.25±0.04%●	98.72±0.06%	92.77±0.23%●	78.74±1.41%●
EXP	99.27±0.01%●	98.38±0.11%●	93.23±0.04%●	79.84±1.22%●
LOG	99.38±0.09%	98.75±0.06%	93.52±0.07%	84.10±0.54%●
MAE	99.29±0.03%●	98.47±0.17%●	90.10±3.41%●	74.05±0.87%●
MSE	98.71±0.03%●	95.53±0.17%●	90.81±0.18%●	79.12±0.40%●
GCE	98.84±0.02%●	97.48±0.16%●	91.72±0.08%●	79.47±0.38%●
Phuber-CE	97.31±0.07%●	92.44±1.19%●	88.94±0.11%●	70.73±0.39%●

- PL $k$ NN [25]: It adapts the widely-used  $k$ -nearest neighbors method to make predictions for partially labeled examples.

For all the above methods, their parameters are specified or searched according to the suggested parameter settings by respective papers. It is worth noting that since all the compared PLL methods use full batch size, we also use full batch size (with 2000 training epochs) for our proposed methods RC and CC, to keep fair comparisons.

Besides, we also compare with various complementary-label learning methods for two reasons: 1) By regarding each non-candidate label as a complementary label, we can transform the partially labeled dataset into complementarily labeled dataset, thus we can directly use complementary label methods. 2) Existing complementary-label learning methods can be applied to deal with large-scale datasets. The compared complementary-label learning methods are listed as follows.

- PC [9]: It utilizes the pairwise comparison strategy (with sigmoid loss) in the multi-class loss function to learn from complementarily labeled data.
- Forward [36]: It conducts forward correction by estimating the latent class transition probability matrix to learn from complementarily labeled data.
- Free, NN, GA [10]: These are three methods adapted from the same unbiased risk estimator for learning from complementarily labeled data. For the Free method, it minimizes the original empirical risk estimator. For the NN method, it corrects the negative term in the risk estimator using max operator. For the GA method, it uses a gradient ascent strategy to prevent from overfitting.
- MAE, MSE, GCE, Phuber-CE [37]: These are four methods that insert conventional bounded multi-class loss functions into the unbiased risk estimator for learning with multiple complementary labels.
- EXP, LOG [37]: They are two methods for learning with multiple complementary labels. For these two methods, upper-bound surrogate loss functions are used in the derived empirical risk estimator [37].

Hyper-parameters for all the methods are selected so as to maximize the accuracy on a validation set, which is constructed by randomly sampling 10% of the training set.

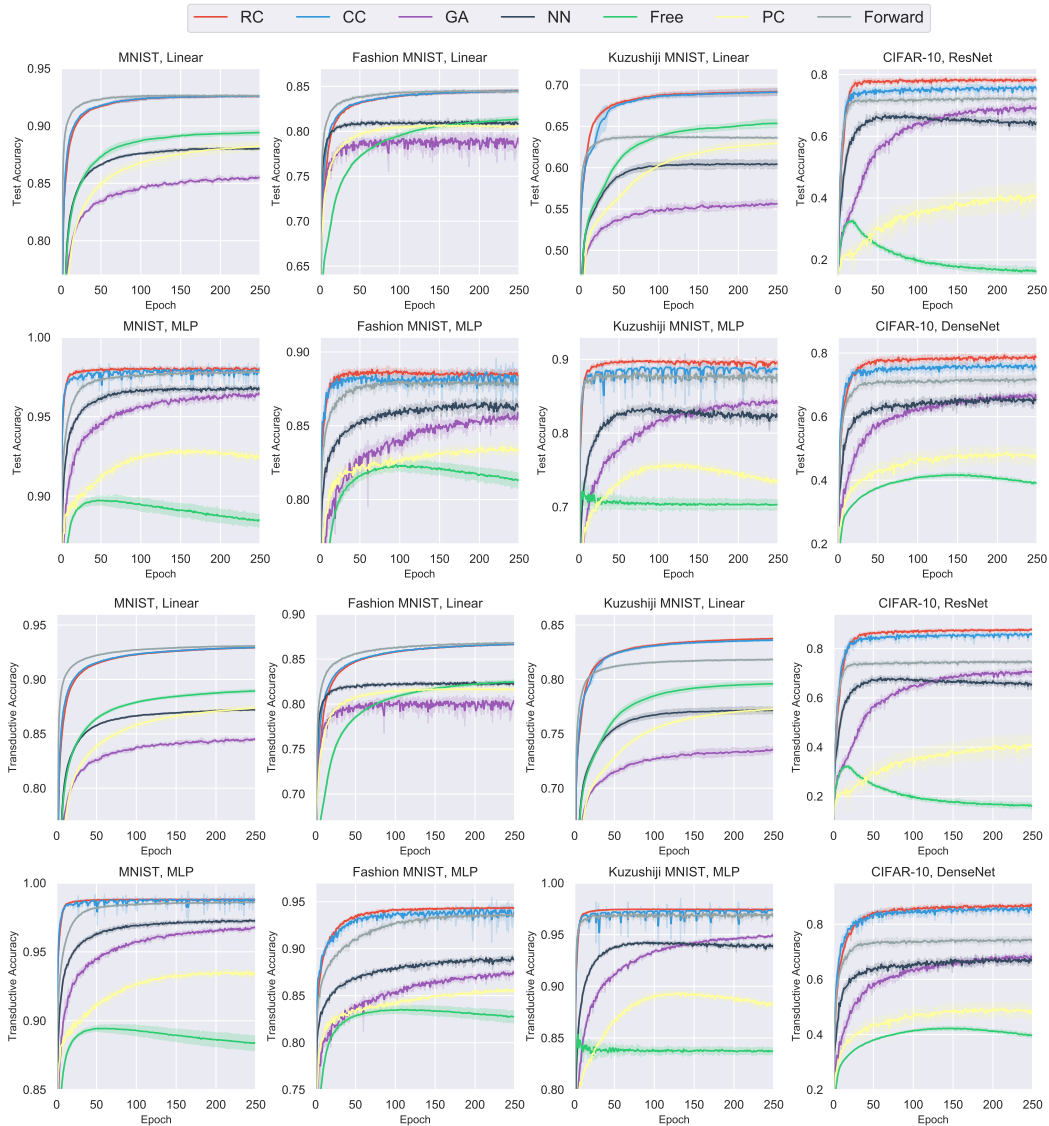


Figure 1: Experimental results of different methods for different datasets and models. Dark colors show the mean accuracy of 5 trials and light colors show the standard deviation.

### E.3 Transductive Analysis

Here, we provide additional experiments to investigate the transductive accuracy of each method, i.e., the training set is evaluated with true labels. Table 7 and Table 8 report the transductive accuracy of each method using different neural networks on benchmark datasets. As shown in the two tables, our proposed methods RC and CC still significantly outperform other compared methods in most cases. In addition, it is worth noting that the gap of transductive accuracy between RC and CC is not so significant. However, as shown before, the gap of test accuracy between RC and CC is quite significant. These observations further



Table 9: Test performance (mean $\pm$ std) of the RC method using neural networks on benchmark datasets with different generation models. The best performance is highlighted in bold.

	Case 1	Case 2	Case 3	Case 4	Case 5	Our Case	Supervised
MLP MNIST	95.29● ( $\pm 0.14$ )	97.17● ( $\pm 0.04$ )	97.68● ( $\pm 0.10$ )	97.93 ( $\pm 0.15$ )	98.97 ( $\pm 0.12$ )	<b>98.00</b> ( $\pm 0.11$ )	<u>98.48</u> ( $\pm 0.00$ )
MLP KMNIST	79.88● ( $\pm 0.47$ )	85.65● ( $\pm 0.38$ )	88.04● ( $\pm 0.37$ )	89.07● ( $\pm 0.20$ )	89.34 ( $\pm 0.18$ )	<b>89.38</b> ( $\pm 0.21$ )	<u>91.53</u> ( $\pm 0.00$ )
MLP FMNIST	79.78● ( $\pm 0.32$ )	84.97● ( $\pm 0.32$ )	87.05● ( $\pm 0.17$ )	88.09● ( $\pm 0.18$ )	88.27 ( $\pm 0.24$ )	<b>88.38</b> ( $\pm 0.23$ )	<u>89.37</u> ( $\pm 0.00$ )
LeNet MNIST	98.82● ( $\pm 0.05$ )	99.02 ( $\pm 0.06$ )	99.02 ( $\pm 0.06$ )	<b>99.04</b> ( $\pm 0.08$ )	<b>99.04</b> ( $\pm 0.05$ )	<b>99.04</b> ( $\pm 0.08$ )	<u>99.22</u> ( $\pm 0.00$ )
LeNet KMNIST	92.81● ( $\pm 0.39$ )	93.54● ( $\pm 0.21$ )	93.71● ( $\pm 0.20$ )	93.77● ( $\pm 0.23$ )	93.89 ( $\pm 0.25$ )	<b>94.00</b> ( $\pm 0.31$ )	<u>95.34</u> ( $\pm 0.00$ )
LeNet FMNIST	81.59● ( $\pm 0.18$ )	86.49● ( $\pm 0.31$ )	88.48● ( $\pm 0.15$ )	89.24● ( $\pm 0.11$ )	89.45 ( $\pm 0.18$ )	<b>89.48</b> ( $\pm 0.11$ )	<u>89.93</u> ( $\pm 0.00$ )

Table 10: Test performance (mean $\pm$ std) of the CC method using neural networks on benchmark datasets with different generation models. The best performance is highlighted in bold.

	Case 1	Case 2	Case 3	Case 4	Case 5	Our Case	Supervised
MLP MNIST	96.36● ( $\pm 0.17$ )	97.49● ( $\pm 0.10$ )	97.76 ( $\pm 0.12$ )	97.85 ( $\pm 0.08$ )	<b>97.87</b> ( $\pm 0.17$ )	<b>97.87</b> ( $\pm 0.10$ )	<u>98.48</u> ( $\pm 0.00$ )
MLP KMNIST	80.65● ( $\pm 0.86$ )	86.43● ( $\pm 0.80$ )	88.06● ( $\pm 0.57$ )	88.69 ( $\pm 0.21$ )	88.73 ( $\pm 0.44$ )	<b>88.83</b> ( $\pm 0.40$ )	<u>91.53</u> ( $\pm 0.00$ )
MLP FMNIST	79.81● ( $\pm 0.45$ )	84.49● ( $\pm 0.33$ )	86.47● ( $\pm 0.14$ )	87.52● ( $\pm 0.15$ )	87.64 ( $\pm 0.18$ )	<b>87.80</b> ( $\pm 0.25$ )	<u>89.37</u> ( $\pm 0.00$ )
LeNet MNIST	98.28● ( $\pm 0.19$ )	98.83● ( $\pm 0.08$ )	98.93 ( $\pm 0.07$ )	98.94 ( $\pm 0.02$ )	98.95 ( $\pm 0.09$ )	<b>98.99</b> ( $\pm 0.08$ )	<u>99.22</u> ( $\pm 0.00$ )
LeNet KMNIST	86.67● ( $\pm 1.22$ )	92.16● ( $\pm 0.30$ )	93.13● ( $\pm 0.26$ )	93.41● ( $\pm 0.30$ )	93.81 ( $\pm 0.22$ )	<b>93.86</b> ( $\pm 0.18$ )	<u>95.34</u> ( $\pm 0.00$ )
LeNet FMNIST	77.75● ( $\pm 5.32$ )	86.11● ( $\pm 0.31$ )	87.86● ( $\pm 0.20$ )	88.53● ( $\pm 0.31$ )	88.97 ( $\pm 0.25$ )	<b>88.98</b> ( $\pm 0.20$ )	<u>89.93</u> ( $\pm 0.00$ )

support our conjecture that the estimation error bound of RC is probably tighter than that of CC.

## E.4 Performance Curves

Here, we record the test accuracy at each training epoch to provide more detailed visualized results. To avoid the overcrowding of many curves in a single figure, we only use seven methods including RC, CC, GA, NN, Free, PC, and Forward. The linear model and the MLP model are trained on the benchmark datasets. Figure 1 reports the experimental results of the seven methods for different datasets and models. Dark colors show the mean accuracy of 5 trials and light colors show the standard deviation. As shown in Figure 1, our proposed PLL methods RC and CC still consistently outperform other compared methods, even when the simple linear model is used.

Table 11: Test performance (mean $\pm$ std) of each method using neural networks on benchmark datasets. DenseNet is trained on CIFAR-10, and LeNet is trained on the other three datasets. Candidate label sets are generated by the generation model in Case 1 (entropy=2.015).

	MNIST	Kuzushiji-MNIST	Fashion-MNIST	CIFAR-10
RC	<b>98.82<math>\pm</math>0.05%</b>	<b>92.81<math>\pm</math>0.39%</b>	<b>81.59<math>\pm</math>0.18%</b>	<b>68.18<math>\pm</math>0.60%</b>
CC	98.28 $\pm$ 0.19%●	86.67 $\pm$ 1.22%●	77.75 $\pm$ 5.32%●	56.13 $\pm$ 3.33%●
GA	97.29 $\pm$ 0.19%●	83.79 $\pm$ 0.98%●	70.91 $\pm$ 0.99%●	41.57 $\pm$ 1.35%●
NN	69.51 $\pm$ 2.06%●	51.03 $\pm$ 1.88%●	53.13 $\pm$ 2.04%●	31.54 $\pm$ 1.65%●
Free	15.29 $\pm$ 0.58%●	13.60 $\pm$ 0.37%●	10.58 $\pm$ 0.54%●	12.53 $\pm$ 0.34%●
PC	96.56 $\pm$ 0.25%●	85.60 $\pm$ 0.45%●	80.98 $\pm$ 0.44%●	65.97 $\pm$ 0.39%●
Forward	95.87 $\pm$ 4.82%●	90.83 $\pm$ 0.82%●	59.66 $\pm$ 2.75%●	51.25 $\pm$ 0.49%●
EXP	84.37 $\pm$ 9.30%●	71.10 $\pm$ 5.74%●	59.56 $\pm$ 8.43%●	30.35 $\pm$ 0.38%●
LOG	98.17 $\pm$ 0.10%●	87.85 $\pm$ 0.82%●	77.50 $\pm$ 5.12%●	54.61 $\pm$ 4.04%●
MAE	56.81 $\pm$ 8.36%●	49.78 $\pm$ 9.03%●	36.41 $\pm$ 0.29%●	30.61 $\pm$ 0.43%●
MSE	95.80 $\pm$ 0.24%●	74.95 $\pm$ 0.84%●	58.85 $\pm$ 3.52%●	58.18 $\pm$ 1.25%●
GCE	95.92 $\pm$ 0.09%●	80.49 $\pm$ 1.10%●	72.25 $\pm$ 0.35%●	57.47 $\pm$ 0.59%●
Phuber-CE	79.41 $\pm$ 1.61%●	59.88 $\pm$ 1.06%●	58.65 $\pm$ 1.22%●	57.53 $\pm$ 3.36%●

## F Experiments on Effectiveness of Generation Model

Here, we would like to test the performance of our methods under different data generation processes. As indicated before, our proposed PLL methods are based on the proposed data generation model. Therefore, we would like to investigate the influence of different generation models on our proposed methods. We use *entropy* to measure how well given candidate label sets match the proposed generation model. By this measure, we could know ahead of model training whether to apply our proposed methods or not on a specific dataset. We expect that the higher the entropy, the better the match, thus the better the performance of our proposed methods. To verify our conjecture, we generate various candidate labels sets by different generation models. It is worth noting that the average number of candidate labels (Avg. #CLs) per instance plays an important role in partially labeled datasets. Intuitively, the performance of PLL methods would generally be better if trained on the datasets with smaller Avg. #CLs. The Avg. #CLs of our generation model is 5. Therefore, to keep fair comparisons, the Avg. #CLs of other studied generation models is also kept as 5.

In following experiments, we still focus on the case where the candidate label set is independent of the instance. We additionally introduce the *class transition matrix* (denoted by  $\mathbf{T}$ ) for partially labeled data, where  $T_{ij}$  describes the probability of the label  $j$  being a candidate label given the true label  $i$  for each instance. Intuitively,  $T_{ii} = 1$  always holds since the true label is always a candidate label. In this way, we provide various formulations of the matrix  $\mathbf{T}$  to instantiate different generation models.

The studied generation models are illustrated in Figure 2. As shown in Figure 2, we provide six cases of generation models, and each of them holds a value of entropy. The value of entropy is calculated by the following two steps: 1) The matrix  $\mathbf{T}$  is normalized by  $P_{ij} = T_{ij}/(\sum_j T_{ij})$ ,  $\forall i, j \in [k]$ . 2) The entropy of the case is calculated by  $-\frac{1}{k} \sum_{i=1}^k \sum_{j=1}^k P_{ij} \log P_{ij}$ . As in our proposed generation model, given the true label, other labels have the same probability to be a candidate label, our case achieves the maximum entropy (i.e., 2.257).

Table 9 and Table 10 report the test performance (mean $\pm$ std) of the RC method and the CC method using neural networks on benchmark datasets with different generation models. From the two tables, we can observe that the higher the entropy, the better the match, thus the better the performance of our proposed methods. Thus, our conjecture is clearly validated.

We further conduct experiments with the generation model of Case 1 where given candidate label sets do not match our proposed generation model well. The experimental results are shown in Table 11. As can be seen from Table 11, our proposed methods still significantly outperform other compared methods in most cases, and RC always achieves the best performance.